Article:
Bryant, Dan, Dixon, William, Hopkins, James R. et al. (2019) Strong anthropogenic control of secondary organic aerosol formation from isoprene in Beijing [discussion paper]. Atmospheric Chemistry and Physics Discussions. ISSN: 1680-7367

https://doi.org/10.5194/acp-2019-929

https://doi.org/10.5194/acp-2019-929
Preprint. Discussion started: 23 October 2019

Atmospheric Chemistry and Physics Discussions

Strong anthropogenic control of secondary organic aerosol formation from isoprene in Beijing

Daniel J. Bryant[1], William J. Dixon[1], James R. Hopkins[1,2], Rachel E. Dunmore[1], Kelly L. Pereira[1], Marvin Shaw[1,2], Freya A. Squires[1], Thomas J. Bannan[3], Archit Mehra[3], Stephen D. Worrall[3±], Asan Bacak[3], Hugh Coe[3], Carl J. Percival[3φ], Lisa K. Whalley[2,4], Dwayne E. Heard[2,4], Eloise J. Slater[4], Bin Ouyang[5,6], Tianqu Cui[7], Jason D. Surratt[7], Di Liu[8], Zongbo Shi[8,9], Roy Harrison[8], Yele Sun[10], Weiqi Xu[10], Alastair C. Lewis[1,2], James D. Lee[1,2], Andrew R. Rickard[1,2], Jacqueline F. Hamilton[1]

[1] Wolfson Atmospheric Chemistry Laboratories, Department of Chemistry, University of York, York, UK
[2] National Centre for Atmospheric Science, University of York, York, UK
[3] School of Earth and Environmental Sciences, The University of Manchester, Manchester, UK
[4] School of Chemistry, University of Leeds, Leeds, UK
[5] Lancaster Environment Centre, Lancaster University, Lancaster, UK
[6] Department of Chemistry, University of Cambridge, Cambridge, UK
[7] Department of Environmental Sciences and Engineering, Gillings School of Global Health, University of North Carolina, Chapel Hill, USA
[8] School of Geography Earth and Environmental Sciences, the University of Birmingham, Birmingham, UK
[9] Institute of Surface-Earth System Science, Tianjin University, Tianjin, China
[10] Institute of Atmospheric Physics, Chinese Academy of Sciences, Beijing, People's Republic of China

± Now at Chemical Engineering and Applied Chemistry, School of Engineering and Applied Science, Aston University, Birmingham, UK
φ Now at Jet Propulsion Laboratory, California Institute of Technology, 4800 Oak Grove Drive, Pasadena, CA, USA

Correspondence to: Jacqueline Hamilton (jacqui.hamilton@york.ac.uk)

Abstract: Isoprene-derived secondary organic aerosol (iSOA) is a significant contributor to organic carbon (OC) in some forested regions, such as tropical rainforests and the Southeast US. However, its contribution to organic aerosol in urban areas, with high levels of anthropogenic pollutants, is poorly understood. In this study we examined the formation of anthropogenic-influenced iSOA during summer in Beijing, China. Local isoprene emissions and high levels of anthropogenic pollutants, in particular NO_X and particulate SO_4^{2-}, led to the formation of iSOA under both high- and low-NO oxidation conditions, with significant heterogeneous transformations of isoprene-derived oxidation products to particulate organosulfates (OSs) and nitrooxy-organosulfates (NOSs). Ultra-pressure liquid chromatography coupled to high-resolution mass spectrometry was combined with a rapid automated data processing technique to quantify 31 proposed iSOA tracers in offline $PM_{2.5}$ filter extracts. The co-elution of the inorganic ions in the extracts caused matrix effects that impacted two authentic standards differently. The average concentration of iSOA OSs and NOSs was 82.5 ng m^{-3}, around three times higher than the observed concentrations of their oxygenated precursors (2-methyltetrols and 2-methylglyceric acid). OS formation was dependant on both photochemistry and sulfate available for reactive uptake as shown by a strong correlation with the product of ozone (O_3) and particulate sulfate (SO_4^{2-}). A greater proportion of high-NO OS products were observed in Beijing compared to previous studies in less polluted environments. The iSOA derived OSs and NOSs represented on average 0.62 %

https://doi.org/10.5194/acp-2019-929
Preprint. Discussion started: 23 October 2019

Atmospheric Chemistry and Physics Discussions

of the oxidised organic aerosol measured by aerosol mass spectrometry, but this increased to ~3 % on certain days. These results indicate for the first time that iSOA formation in urban Beijing is strongly controlled by anthropogenic emissions and results in extensive conversion to heterogeneous OS products.

1 Introduction

Rapidly developing countries such as China often experience very poor air quality. Beijing regularly experiences periods of very high particle pollution, with annual and 24-hourly levels well above World Health Organisation guidelines (Chan et al., 2008; Hu et al., 2014). Premature mortality, as a result of respiratory illness, cardiovascular disease and cancer, has been associated with exposure to poor air quality (Dockery et al., 1993; Pope et al., 2000, 2006; Jerrett et al., 2009; Beelen et al., 2014; Laurent et al., 2014; Ostro et al., 2015). Lelieveld et al. (2015) estimated that 1.36 million premature deaths in China in 2010 were a result of exposure to outdoor air pollution. By far the most dangerous pollutant to health in China are particles less than 2.5 microns in diameter, known as $PM_{2.5}$, with a recent study suggesting that a 50 % reduction in excess mortality requires a 62 % reduction in $PM_{2.5}$ in the Beijing-Tianjin-Hebei (BTH) region (Hu et al., 2017a).

Previous measurements using aerosol mass spectrometry (AMS) indicate that PM_1 in Beijing is mainly composed of sulfate, nitrate, ammonium and organics (Hu et al., 2016. Zhang et al., 2013). Positive Matrix Factorisation of AMS measurements indicate that oxidised or secondary organic aerosol (SOA) can make up a substantial fraction of the PM_1 mass (> 25 %), even in urban areas, but the sources of this material are still poorly understood (Zhang et al., 2011; Sun et al., 2018). Hu et al. (2017a) estimated that exposure to SOA was responsible for 0.14 million deaths in China in 2013 based on mass contribution alone, ranging from < 1 % to 23 % source contributions to $PM_{2.5}$ depending on location. Zhang et al. (2017) used ^{14}C measurements to determine that non-fossil emissions are generally a dominant contributor of secondary organic carbon (SOC) in Beijing, with a larger contribution in summer as a result of increased biogenic volatile organic compounds (VOCs) emissions.

Hu et al. (2017b) updated the Community Multi-scale Air Quality (CMAQ) model with updated SOA yields and a more detailed description of SOA formation from isoprene oxidation. Removing all anthropogenic pollutants from the model resulted in a huge drop in isoprene SOA concentrations, indicating that controlling anthropogenic emissions would result in reduction of both anthropogenic and biogenic SOA. The predicted SOA was dominated by isoprene in summer across China and in four cities (Beijing, Guangzhou, Shanghai, Chengdu) with concentrations up to 30 μg m^{-3} in Beijing. However, there is currently very little observational evidence to support such high SOA mass concentrations from isoprene oxidation in these Chinese cities. The widely used SOA tracer method (Kleindienst et al., 2007) has been used extensively to estimate the fraction of isoprene-derived SOA (iSOA) across China. Ding et al. (2014) studied SOA at 14 Chinese sites and found that iSOA dominated the apportioned SOA mass (46 ± 14 %), with it contributing between 0.4 – 2.17 μg m^{-3} and an average of 1.59 μg m^{-3} in Beijing. However, only a very limited subset of VOC precursors was included, and this method fails to account for heterogeneous formation processes. To overcome some of these limitations, Wang et al. (2017) used

https://doi.org/10.5194/acp-2019-929
Preprint. Discussion started: 23 October 2019

Atmospheric Chemistry and Physics Discussions

tracer-based source apportionment of $PM_{2.5}$ with positive matrix factorisation in the Pearl River Delta region during summer. They identified an iSOA factor that contributed up to 4 μg m^{-3} in Guangzhou, and up to 11 % of the total SOC.

A multitude of studies have examined iSOA formation (Pandis et al., 1991; Edney et al., 2005; Kroll et al., 2006; Dommen et al., 2006; Kleindienst et al., 2006; Ng et al., 2006; Surratt et al., 2007a, 2007b, 2008, 2010; Ng et al., 2008; Paulot et al., 2009; Chan et al., 2010; Chhabra et al., 2010; Nguyen et al., 2011, 2014, 2015; Zhang et al., 2011, 2012; Lin et al., 2013; Xu et al., 2014; Krechmer et al., 2015; Clark et al., 2016; Riva et al., 2016a, 2016b); however, the magnitude of iSOA formed can be vastly different from study to study (Carlton et al., 2009). Furthermore, there have been limited field measurements to establish if these estimates are representative of urban environments (Wang et al., 2018; Li et al., 2018; Glasius et al., 2018; Le Breton et al., 2018; Hettiyadura et al., 2018,2019; Rattanavaraha et al., 2016; Budisulistiorini et al., 2013).

iSOA formation during the daytime is dominated by reaction with hydroxyl radicals (OH), with the concentrations of NO having a strong influence on the reaction products (Wennberg et al., 2018 and references therein). Under low-NO conditions the isoprene peroxyradicals (RO_2) can react with hydroperoxy radicals (HO_2) to form isoprene hydroxyhydroperoxides (ISOPOOH). The ISOPOOH isomers can react further with OH to form isoprene epoxydiol isomers (β− or δ-IEPOX) (Paulot et al., 2009), which can undergo uptake into acidified sulfate particles to form 2-methyltetrol organosulfates (2-MT-OS) (Surratt et al., 2010. Lin et al., 2012). Under high-NO conditions, isoprene RO_2 can react with NO to form alkoxy radicals (RO) producing methacrolein (MACR) and methyl vinyl ketone (MVK) as the main reaction products. The reaction of MACR with OH, and subsequent addition of NO_2, leads to the methylacrloylperoxynitrate (MPAN), which reacts with OH to produce hydroxymethylmethyl-α-lactone (HMML) (Nguyen et al., 2015) or methyacrylic epoxide (MAE) (Lin et al., 2013). HMML is thought to be the more abundant product compared to MAE (Nguyen et al., 2015). Subsequent uptake of HMML into wet sulfate aerosols is proposed to lead to either 2-methylglyceric acid (2-MG) or its organosulfate derivative (2-MG-OS), as well as their dimers and higher order oligomers (Surratt et al., 2006; Surratt et al., 2010; Lin et al., 2013; Nguyen et al., 2015). Recently Schwantes et al. (2019) showed that under ambient conditions the formation of SOA from low-volatility nitrates and dinitrates, formed via reactions of isoprene derived RO_2 with NO, is also important. Chamber-derived SOA yields for OH chemistry are variable depending on the experimental conditions, but are generally low (<10 %). The addition of acidified sulfate aerosol, accounting for wall losses and using more atmospherically relevant radical lifetimes can lead to significantly higher SOA yields in chamber studies (Surratt et al., 2010; Lin et al. 2012; Gaston et al., 2014). However, recent work has revealed that isoprene SOA formation can be suppressed when viscous organic coatings are present on acidified sulfate aerosol, impeding the multiphase chemistry of IEPOX yielding additional SOA (Riva et al., 2016b; Zhang et al., 2018; Riva et al., 2019).

https://doi.org/10.5194/acp-2019-929
Preprint. Discussion started: 23 October 2019

Atmospheric Chemistry and Physics Discussions

Observations using aerosol mass spectrometry (AMS) indicate that IEPOX-derived SOA can make up a significant fraction of organic aerosol in isoprene-rich environments, such as Borneo (23 %; Robinson et al., 2011), the Amazon (34 %; Chen et al., 2015) and the South East US (33-40 %; Budisulistiorini et al., 2013; Budisulistiorini et al., 2016; Rattanvaraha et al., 2017). Hu et al. (2015) compared previous AMS studies and found a magnitude lower average IEPOX-SOA signal in urban studies (f_{C5H6O} = 0.17 %) compared to those in isoprene-rich regions (f_{C5H6O} = 2.2 %). The average IEPOX-SOA concentration measured in Nanjing, a polluted city in Eastern China, in August 2013 was 0.33 μg m^{-3} (Zhang et al., 2017). This represented only 3.8 % of the total OA, indicating there is limited formation of IEPOX under high-NO_x conditions (average NO_x = 21 ppb). He et al. (2018) found higher concentrations of the low-NO isoprene SOA tracers (average = 121 ng m^{-3}) than the high-NO iSOA tracers (average = 9 ng m^{-3}) at a regional background site (Wanqingsha) situated within the heavily polluted Pearl River Delta Region. Only two high-NO iSOA tracers were measured (2-MG and 2-MG-OS), which could lead to a significant underestimate of the strength of the high NO_x pathway. Wang et al. (2018) measured a range of OSs at a regional site 38 km north east of Beijing during May-June 2016. Isoprene-derived OSs ranged from 0.9-20 ng m^{-3}, with a mean isoprene-derived OS concentration of 14.8 ng m^{-3}. In both these studies, the ratio of the average concentration of the commonly used OS tracers from the low NO versus the high NO pathways was close to 1.5 (2-MT-OS:2-MG-OS; Beijing = 1.47, Wanqingsha = 1.57) indicating that even in polluted environments low-NO oxidation chemistry can play a significant role in iSOA formation.

The lack of molecular-level measurements of iSOA in highly polluted urban areas makes it difficult to determine the role of isoprene in summer haze episodes in Beijing. To investigate the formation of iSOA in Beijing, offline $PM_{2.5}$ filter samples were collected during summer 2017 as part of the Atmospheric Pollution and Human Health program (Shi et al., 2019). The filters were extracted and then screened using a sensitive and selective high throughput method based on ultra performance liquid chromatography coupled to ultra-high resolution mass spectrometry equipped with electrospray ionization (UPLC/ESI-HR-MS). High-time resolution filter sampling allowed the formation and evolution of iSOA to be studied, with observed concentrations strongly controlled by levels of anthropogenic pollutants.

2 Experimental

2.1 $PM_{2.5}$ filter sampling and extraction

Aerosol samples were collected between the 18th May and 24th June 2017 at the Institute of Atmospheric Physics (IAP) in Beijing, China. This sampling was part of the Sources and Emissions of Air Pollutants in Beijing (AIRPOLL-Beijing) project, as part of the wider Atmospheric Pollution and Human Health in a Chinese Megacity (APHH-Beijing) programme (Shi et al., 2019). $PM_{2.5}$ filter samples were collected using an ECOTECH HiVol 3000 (Ecotech, Australia) high-volume air sampler with a selective $PM_{2.5}$ inlet, with a flow rate of 1.33 m^3 min^{-1}. Filters were baked at 500 ºC for five hours before use. After collection, samples were wrapped in foil, and then stored at -20 ºC and shipped to the laboratory for offline analysis. Samples were collected at a height of 8 m, on top of a building in the IAP complex.

https://doi.org/10.5194/acp-2019-929
Preprint. Discussion started: 23 October 2019

Atmospheric Chemistry and Physics Discussions

Samples were collected every 3 hours during the day, approximately between 08:30 and 17:30 and then one sample was collected overnight between 17:30 and 08:30. Hourly samples were also taken on certain days towards the end of the sampling period on high pollution days. 24-hour samples were also collected using a Digitel high volume $PM_{2.5}$ sampler at the same location.

The extraction of the organic aerosol from the filter samples was based on the method in Hamilton et al., (2008). Initially, an 8^{th} of the filter was cut up into roughly 1 cm^2 pieces and stored in a vial. 4 ml of LC-MS grade H_2O was then added to the sample and left for two hours. The samples were then sonicated for 30 minutes. Using a 2 ml syringe, the water extract is then pushed through a 0.22 µm filter (Millipore) into another sample vial. An additional 1 mL of water was added to the filter sample, then extracted through the filter, to give a combined aqueous extract. This extract was then reduced to dryness using a vacuum solvent evaporator (Biotage, Sweden). The dry sample was then reconstituted in 1 mL 50:50 MeOH:H_2O solution for offline chemical analysis.

2.2 Ultra-performance liquid chromatography tandem mass spectrometry (UPLC-MS^2)

The extracted filter samples and standards were analysed using UPLC-MS^2, using an Ultimate 3000 UPLC (Thermo Scientific, USA) coupled to a Q-Exactive Orbitrap MS (Thermo Fisher Scientific, USA) with a heated electrospray ionisation (HESI). The UPLC method uses a reverse phase 5 µm, 4.6 x 100mm, Accucore column (Thermo Scientific, UK) held at 40 ºC. The mobile phase consists of LC-MS grade water and 100 % MeOH (Fisher Chemical, USA). The water was acidified using 0.1 % formic acid to improve peak resolution. The injection volume was 2 µL. The solvent gradient was held for a minute at 90:10 H_2O:MeOH, then changed linearly to 10:90 H_2O:MeOH over 9 minutes, then held for 2 minutes at this gradient before returning to 90:10 H_2O:MeOH over 2 minutes and then held at 90:10 for the remaining 2 minutes, with a flow rate of 300 µL min^{-1}. The mass spectrometer was operated in negative mode using full scan MS^2. The scan range was set between 50 - 750 m/z. The ESI voltage was 4 kV, with capillary and auxiliary gas temperatures of 320 ºC. The samples were run in batches of 70, in a repeating sequence of 5 samples followed by one blank. The calibrations were run separately after the samples were finished, in the following sequence; (3 X same concentration) X number of standards in calibration curve from the lowest concentration to the highest followed by 2 blanks. The quantification method will be discussed in the results section.

2.3 Construction of accurate mass library

A mass spectral library was built using the compound database function in TraceFinder 4.1 General Quan software (Thermo Fisher Scientific, USA). Each compound was input into the compound library in the generic form: $C_cH_hO_oN_nS_s$ (where c, h, o, n, and s represent the number of carbon, hydrogen, oxygen, nitrogen and sulfur atoms respectively). From literature, species were identified, searched for in the ambient samples according to their accurate mass, and then the retention time (RT) of each isomer was obtained. The accurate masses, RT and literature references for iSOA tracers are shown in Table 1.

2.4 Automated method for SOA tracer analysis

https://doi.org/10.5194/acp-2019-929
Preprint. Discussion started: 23 October 2019

Atmospheric Chemistry and Physics Discussions

The UPLC/ESI-HR-MS data for each ambient sample and standard was analysed using TraceFinder™. The mass tolerance of the method was set to 2 ppm and the retention time window was set to 30 s, although for species with multiple isomers present, the integration was checked to make sure the same peaks were not being integrated twice, and the window changed accordingly. The peak tailing factor was set to 2.0 to reduce the integration of the peak tails. The minimum signal to noise (S/N) for a positive identification was set to 3.0. Using the output from TraceFinder, an *in-house* R code script was developed to combine the identified species and peak areas with the correct filter sampling date/time midpoint and volume of air sampled. Calibration curves from the standards were then obtained, and the intercept and gradient inputted to quantify the iSOA tracer concentrations in the extract. These quantified values were then converted to the mass on the whole filter and divided by the volume of air sampled for that filter sampling period and converted to units of ng m^{-3}. Higher time resolution data were averaged to the filter sampling times.

2.5 Hydrophilic Liquid Interaction Chromatography (HILIC).

A subset of filters (n=15) were also analysed at the University of North Carolina (UNC) using a newly developed HILIC method interfaced to high-resolution quadrupole time-of-flight mass spectrometry equipped with ESI (i.e., HILIC/ESI-HR-QTOFMS) (Cui et al., 2018). Briefly, filters were extracted with 22 mL of LC/MS-grade methanol by 45 min of sonication; the samples were first extracted for 23 min, the water bath replaced with cool water, and then extracted again for 22 min. This was done to make sure the water bath contained within the sonicator did not reach above 30 C. Extracts were filtered through polypropylene membrane syringe filters in order to remove insoluble filter fibres and soot particles. The extracts were dried under a gentle stream of nitrogen gas. Dried methanol extracts were reconstituted with 150 µL of 95:5 (v/v) LC/MS-grade acetonitrile/Milli-Q water. Operating details of the HILIC/ESI-HR-QTOFMS used for these samples is also summarized by Cui et al. (2018).

2.6 Gas Chromatography – Mass Spectrometer

Details of the measurement procedure used can be found elsewhere (Fu et al., 2010). Briefly, filter samples were extracted with dichloromethane/methanol (2:1 v/v), filtered through quartz wool packed in a Pasteur pipette, concentrated using a rotary evaporator under vacuum, and blown down to dryness with pure nitrogen gas. The extracts were derivatized and diluted with n-hexane containing the internal standard prior to GC-MS analysis. Separation was performed on a fused silica capillary column (DB-5MS: 30 m × 0.25 mm × 0.25 µm). The MS detection was conducted in electron ionization (EI) mode at 70 eV, scanning from 50 to 650 Da. Individual compounds were identified by comparison of mass spectra with those of authentic standards or literature data. 2-methylglyceric acid, C_5-alkene triols (the sum of *cis*-2-methyl-1,3,4-trihydroxy-1-butene, *trans*-2-methyl-1,3,4-trihydroxy-1-butene, and 3-methyl-2,3,4-trihydroxy-1-butene), and 2-methyltetrols (the sum of 2-methylthreitol and 2-methylerythritol) were quantified using the response factor of *meso*-erythritol. Field blank filters were treated as the real samples for quality assurance. Target compounds were not detected in the blanks.

2.7 High-Resolution Aerosol Mass Spectrometry measurements

https://doi.org/10.5194/acp-2019-929
Preprint. Discussion started: 23 October 2019

Atmospheric Chemistry and Physics Discussions

The size-resolved non-refractory submicron aerosol species at the same site were measured by an Aerodyne high-resolution time-of-flight aerosol mass spectrometer (HR-ToF-AMS) at a time resolution of 5 min. The elemental ratios of hydrogen-to-carbon (H:C) and oxygen-to-carbon (O:C) of OA were determined, and the sources of OA were analysed with positive matrix factorisation. Six OA factors were identified in summer including two primary factors; hydrocarbon like OA (HOA), cooking OA (COA), and three oxidised OA factors with increasing degrees of oxidation, OOA1 (O:C = 0.53), OOA2 (O:C = 0.74), OOA3 (O:C = 1.18).

2.8 Iodide CIMS

A time of flight chemical ionisation mass spectrometer (ToF-CIMS) (Lee et al. 2014; Priestley et al. 2018) using an iodide ionisation system coupled with a filter inlet for gases and aerosols (FIGAERO) was deployed here to make near simultaneous, real-time measurements of both the gas- and particle-phase chemical composition. The instrument was originally developed by Lopez-Hilfiker et al. (2014) and is described and characterised in more detail by Bannan et al., (2019). The experimental set up employed by the University of Manchester ToF-CIMS is described in Zhou et al., (2019). Only gas phase data is presented herein.

Field calibrations were regularly carried out using known concentration of formic acid in gas mixtures made in a custom-made gas phase manifold. A range of other species were calibrated for after the campaign, and relative calibration factors were derived using the measured formic acid sensitivity during the in-situ calibrations (Bannan et al. 2015). Offline calibrations after the field work campaign were performed specific to the isoprene oxidation species observed here. IEPOX ($C_5H_{10}O_3$) synthesized by the University of North Carolina, Department of Environmental Sciences & Engineering was specifically calibrated for. Known concentrations were deposited on the FIGAERO filter in various amounts and thermally desorbed using a known continuous flow of nitrogen over the filter. For the isoprene nitrate; $C_5H_9NO_4$ there was no direct calibration source available and concentrations using the calibration factor of $C_5H_{10}O_3$ are presented here.

2.9 Gas-phase measurements

Additional gas-phase measurements were collected at the site from an elevated inlet at 8 m. Data included Nitrogen oxide, NO, measured by chemiluminescence with a Thermo Scientific Model 42i NO_x analyser and Nitrogen dioxide, NO_2, was measured using a Teledyne Model T500U Cavity Attenuated Phase Shift (CAPS) spectrometer. The sum of the NO_y species was measured using a Thermo Scientific Model 42C NO_x analyser and a heated molybdenum converter at the sample inlet. The molybdenum converter reduces NO_y compounds to NO allowing measurement by chemiluminescence. Ozone, O_3, was measured using a Thermo Scientific Model 49i UV photometric analyser. All instruments were calibrated throughout the measurement period, with a 'zero' or 'background' calibration using a Sofnofil/charcoal trap. Span (high concentration) calibrations were carried out using gas standards. Both the Thermo Scientific 42i and 42C instrument calibrations are traceable to the National Physical Laboratories (NPL)

https://doi.org/10.5194/acp-2019-929
Preprint. Discussion started: 23 October 2019

Atmospheric Chemistry and Physics Discussions

NO scale. The meteorological variables of wind speed, wind direction, relative humidity (RH), and temperature were measured at 102 m on the IAP 325 m meteorological tower.

Observations of VOCs were made using a dual-channel GC with flame ionisation detectors (DC-GC-FID). Air was sampled at 30 L min^{-1} at a height of 5m, through a stainless-steel manifold (½" internal diameter). 500 mL subsamples were taken, dried using a glass condensation finger held at -40°C and then pre-concentrated using a Markes Unity2 pre-concentrator on a multi-bed Ozone Precursor adsorbent trap (Markes International Ltd). These samples were then transferred to the GC over for analysis following methods described by Hopkins et al. (2011).

Further details of the following additional gas phase instrumentation can be found in the SI and Shi et al., 2019. Isoprene was also measured at a height of ~102 m using a Voice200 Selected ion flow tube mass spectrometer (SIFT-MS, Syft Technologies, Christchurch, New Zealand). OH, HO_2 and RO_2 concentrations were measured using Fluorescence Assay by Gas Expansion (FAGE) and NO_3 concentrations were measured using Broadband cavity enhanced absorption spectrometry (Zhou et al., 2018).

3 Results and discussion

The field campaign was conducted at the Institute of Physics, Beijing, situated between the third and fourth ring roads (Shi et al., 2019). The site is typical of central Beijing, surrounded by residential and commercial properties and is near several busy roads. It is also close to several green spaces including a tree-lined canal to the south and the Olympic forest park to the north-east, providing sources for local isoprene emissions.

3. 1 Isoprene gas phase concentrations and loss processes

Isoprene was measured hourly using the DC-GC-FID between 18/05/2017 – 20/06/2017 and the observed concentrations are shown in Figure 1, alongside NO, NO_2 and ozone. The mean mixing ratio of isoprene was 0.53 ppb, with a maximum of 2.9 ppb on the 16/06/2017. The ambient temperature ranged from 16 to 38 °C. Day-time isoprene mixing ratios increased with temperature, with all isoprene mixing ratios above 1 ppb occurring when the temperature was > 25 °C. The average diurnal profile of isoprene in Figure 2a shows low values overnight (< 50 ppt), with a rapid increase at 6 am reaching a maximum of around 1 ppb by the afternoon. The mixing ratio rapidly decreased after 18:00 and returned to very low values by around 22:00. There was strong a correlation between the isoprene mixing ratio measured at 8 m by the DC-GC and at 102 m using the SIFT-MS (R^2 = 0.77). The SIFT-MS measurements were therefore used to investigate the correlation with iSOA tracers when no DC-GC data was available.

Using the average observed diurnal profiles of the main atmospheric oxidants, OH, ozone and NO_3 (shown in SI Figure S1), and isoprene (Figure 2a), the isoprene loss rate was calculated (rate of loss = k_{ox}[Oxidant][Isoprene]) and is shown in Figure 3a. The percentage contribution of each oxidant to the

https://doi.org/10.5194/acp-2019-929
Preprint. Discussion started: 23 October 2019

Atmospheric Chemistry and Physics Discussions

average diurnal isoprene loss rate is shown in Figure 3b. During the day, OH is responsible for over 90 % of isoprene loss, with NO_3 becoming relatively more important from 18:00 until around 03:00, although the amount of isoprene available to react rapidly decreased during this time period. OH chemistry is still an important loss route at night (>30 %) owing to night-time OH sources, such as the ozonolysis of alkenes. Loss of isoprene via ozonolysis however is a minor route, contributing <15 %. During the daytime (10:00-15:00), the lifetime of isoprene was on average around 20 minutes, increasing to a maximum of around 6 hours at 03:00. While the high levels of oxidants lead to a short isoprene lifetime during the day, the ambient concentrations of isoprene are still maintained at the ppb level. This indicates that there are significant local emissions of isoprene impacting the measurement site and therefore a high potential for the formation of iSOA in this urban environment.

3.2 Isoprene SOA in Beijing

Using the high throughput screening method described, the peak areas of 31 potential isoprene-derived OSs and NOSs, which are known iSOA tracers, were measured in 132 $PM_{2.5}$ filter extracts. The full list of iSOA tracers, along with their measured *m/z* and molecular formula is shown in Table 1, ordered by descending average concentration (weighted by filter sampling time and reported in ng m^{-3}) during the campaign.

3.3 Quantification of isoprene OS tracers

Initially, two synthesised isoprene-derived OS standards (2-MT-OS and 2-MG-OS, Cui et al., 2018; Rattanavaraha et al., 2016) were used to produce calibration curves. Both standards gave strong linear calibration curves (R^2 = 0.980 and 0.996 respectively) across an appropriate range of concentrations for the peak areas in the samples. The gradient obtained for the 2-MT-OS standard was ~4 times higher than that of the 2-MG-OS, as shown in Figure S2 To investigate the potential for matrix effects from the large amounts of inorganic sulfate, nitrate and other particulate components that co-elute due to the poor retention of OS in reverse phase UPLC, standard addition calibrations were used. Five-point standard addition calibrations were run on 6 different filter extracts, covering both day and nighttime samples. 50 µL of filter sample extract and 50 µL of the calibrant solution were combined, giving a dilution factor of 2. The five-point calibration range of standard added to each sample was between 0-3 ppm for 2-MGOS and 0-1 ppm for 2-MT-OS. Two examples of the standard addition calibrations are shown in SI Figures S3 (2-MG-OS) and S4 (2-MT-OS), with good linear fits observed (R^2 = 0.997 and 0.997 respectively). A strong matrix effect was observed for the 2-MT-OS, with the concentration measured by standard addition calibration 8.6 to 10 times higher than when using the external calibration carried out on the same day. In contrast, the 2-MG-OS showed a much lower matrix effect, with the concentrations only 1.1-1.5 times higher when using the standard addition calibration. A further comparison using camphorsulfonate, which has a longer retention time (3.74 min) and so does not experience high inorganic ion concentrations in the source, showed no matrix effects when using standard addition. SI Tables 1 and 2 shows a comparison of the concentrations calculated from the standard additions and the two external calibrations.

https://doi.org/10.5194/acp-2019-929
Preprint. Discussion started: 23 October 2019

Atmospheric Chemistry and Physics Discussions

It is not realistic to carry out standard addition calibrations for all samples and all SOA tracers. When the 2-MG-OS external calibration was used to predict the 2-MT-OS concentrations during the standard addition experiments, the concentrations were within a factor of 1.5-2.5. Therefore, the 2-MG-OS external calibration was used as a proxy for all isoprene SOA tracers, with scaling factors applied to account for matrix effects (1.33 for 2-MG-OS, 2.33 for 2-MT-OS, and an average of 1.83 used for all other OSs). Therefore, we estimate an uncertainty on our measured concentrations of 60%. The dinitrate and trinitrate NOS species eluted after the sulfate peak (R_t >1.6 min). In the absence of authentic standards for these species, camphorsulfonate was used as a proxy for calibration. This work highlights an additional difficulty of calibration when using ESI-MS to study OSs and indicates that future studies using reversed phase LC (RPLC) should consider the impacts of matrix effects.

3.4 Organosulfates

3.4.1 2-methyltetrol OS (2-MT-OS)

The 2-MT-OS ($C_5H_{12}SO_7$) formed from the uptake of IEPOX into the particle phase is often used as a marker of low-NO isoprene photochemistry (Wennberg et al., 2018). The time series of 2-MT-OS is shown in Figure 4a. The particle concentration ranged from 0.7 ng m^{-3} to a maximum of 111 ng m^{-3}, with a mean concentration of 11.8 ng m^{-3}. The mean concentrations of 2-MT-OS and 2-MG-OS are compared to observations in previous studies in Table 2. The mean concentration observed in Beijing was much lower than those observed in the Amazon (Riva et al., 2019) and the SE US (Budisolistiorini et al., 2015; Hettiyadura et al., 2019) but are higher than summer time observations at polluted regional background sites in China (Wang et al., 2018; He et al., 2018). The lower amounts of IEPOX-derived SOA results in an average AMS f_{C5H6O} in Beijing during the APHH project of only 0.2 %, similar to observations in other urban studies (Hu et al., 2015).

Hourly samples were collected on selected high pollution days and used to obtain information on the diurnal evolution of the iSOA tracers. The findings on these days are consistent with the three-hourly data. The particulate 2-MT-OS measured by UPLC-MS, on the 11th - 12th June 2017, had a strong diurnal profile (Figure 2b), peaking in the late afternoon, between 15:30 and 18:30, with a minimum over-night. This is consistent with the average diurnal profile of the gas phase precursors IEPOX+ISOPOOH ($C_5H_{12}O_3$) measured using the I^--CIMS (SI Figure S5). High levels of ozone were observed in the afternoon (up to 180 ppb), leading to relatively low levels of NO observed for a highly polluted environment, in some cases below 500 ppt. Thus, although the mixing ratio of NO_x was high, on most afternoons less than 2 % was in the form of NO. High levels of peroxy radicals were observed, with mean afternoon concentrations of HO_2 and RO_2 of around 3 x 10^8 molecule cm^{-3} and 1.5 x 10^9 molecule cm^{-3}, respectively. Zero-dimensional box modelling indicates on some days up to 35 % of the isoprene-derived RO_2 radicals can react with HO_2 in the afternoon (Newland et al., 2019). Thus, the diurnal profile seen in Figure 2b, measured in samples during the measurement period suggests that IEPOX was formed at this urban location by the reaction of OH with local isoprene emissions, with a fraction of the RO_2 radicals formed reacting with HO_2 rather than NO, and subsequent uptake to aerosol forming 2-MT-OS. OH + isoprene hydroxynitrate also has a small yield of IEPOX (Jacobs et al., 2014). The average diurnal

https://doi.org/10.5194/acp-2019-929
Preprint. Discussion started: 23 October 2019

Atmospheric Chemistry and Physics Discussions

profile of isoprene hydroxynitrates ($C_5H_9NO_4$) in the gas phase measured using the I^--CIMS peaks at around 11:00-12:00 followed by a reduction during the afternoon into the evening/night (SI Figure S6). This is likely to be a result of the relatively low levels of NO during the afternoon, which will reduce isoprene nitrate formation from RO_2 + NO reactions, thus isoprene hydroxynitrates are unlikely to be a significant source of 2-MT-OS in Beijing.

The 2-MT-OS showed a moderate correlation with particulate sulfate (R^2=0.44), and a weak anti-correlation with photochemical age, estimated using the ratio of NO_x/NO_y (R^2=0.23). All correlations between species are shown in SI Figure S7. By taking the product of the concentration of ozone, as a proxy of photochemistry, with the amount of particulate sulfate measured using AMS, $[O_3][pSO_4]$, a much stronger correlation with 2-MT-OS was observed (R^2=0.61) as shown in Figure 5. This observation highlights the role of both local photochemistry and particulate sulfate mass in the formation of 2-MT-OS (Figure 5). The correlation of $[O_3][pSO_4]$ with 2-MT-OS is likely to be weaker at longer photochemical ages when the ozone concentration is not directly related to the photochemical formation of the OS. Again, this highlights the strong role of local photochemistry in the production of low-NO iSOA (2-MT-OS) in Beijing. Elevated levels of 2-MT-OS were observed at the start and end of the measurement period which were influenced by strong south-westerly winds. There were also elevated isoprene concentrations (up to 2.9 ppb) and high particulate SO_4^{2-} levels. Therefore, these spikes in 2-MT-OS could be a result of either higher 2-MT-OS in regional aerosol transported to the site or a high isoprene emission source to the south west of the site (i.e. producing IEPOX locally) that then reacts with increased regional sulfate pollution.

Analysis of the 2-MT-OS isomer distribution using HILIC/ESI-HR-QTOFMS, on a subset of 15 samples, indicates that β-IEPOX is the dominant ambient IEPOX isomer, in line with other recent observations (Cui et al, 2018; Krechmer et al., 2016) see SI Figure S8). The MT-OS derived exclusively from δ-IEPOX-OS isomers could not be observed in any of the samples. The 4 IEPOX-OS isomers in SI Figure S8 showed similar temporal trends although small changes in the relative proportions were observed.

3.4.2 2-methyl glyceric acid OS (2-MG-OS)

The most common targeted SOA tracer for high-NO isoprene chemistry is 2-methylglyceric acid (2-MG) and its derivatives. Two observed SOA tracers related to this chemistry are the OS derivatives of 2-methylglyceric acid (2-MG-OS) and the unresolved C_8 dimers of 2-MG-OS ($C_8H_{14}SO_{10}$) that have been identified previously in chamber-derived iSOA (Surratt et al., 2006; Surratt et al., 2010). 2-MG-OS had an average concentration during the campaign of 21.5 ng m^{-3}, ranging from 0.3 to 180.5 ng m^{-3}, with the time series shown in Figure 4b. These values are within the range of 2-MG-OS measured in other urban locations (Nguyen et al., 2014; Rattanavaraha et al., 2016; Hettiyadura et al., 2019). However these concentrations are considerably higher than previously observed at two Chinese polluted regional sites (Wang et al., 2018; He et al., 2018). At these locations, the ratio of the low-NO to high-NO isoprene OS tracer average concentrations was close to 1.5 (2-MT-OS:2-MG-OS; Beijing = 1.47, Wanqingsha = 1.57). However, in central Beijing, this ratio was considerably lower (2-MT-OS:2-MG-OS = 0.55),

https://doi.org/10.5194/acp-2019-929
Preprint. Discussion started: 23 October 2019

Atmospheric Chemistry and Physics Discussions

reflecting the higher proportion of RO_2 radicals reacting with NO at this location compared to the regional measurements. The ratio of 2-MT-OS:2-MG-OS observed in Beijing is compared to previous studies in Table 2 and is considerably lower than measurements taken in a range of isoprene dominated environments (South East US, 2-MT-OS:2-MG-OS = 17, Budisolistiorini et al., 2015.; Amazon, 2-MT-OS:2-MG-OS = 13-118, Glasius et al., (2018).; Atlanta, 2-MT-OS:2-MG-OS = 33, Hettiyadura et al., (2019)) reflecting the strong impact of urban NO emission on iSOA formation.

The mean concentration of the 2-MG-OS dimer ($C_8H_{14}SO_{10}$) was 0.57 ng m^{-3}. A strong linear relationship was observed between the 2-MG-OS monomer and dimer concentrations (R^2=0.83) with a dimer:monomer ratio of 0.02. Formation of oligomers from reactions of 2-MG and HMML has been shown to be reduced in chamber experiments under humid conditions (Schwantes et al., 2019; Nestorowicz et al., 2018). The average RH during the afternoon of the campaign was ~40 %, which may account for the relatively low formation of the dimer OS compared to the monomer (see SI Figure 9).

The diurnal profile of the 2-MG-OS as shown in SI Figure 10 was similar to the 2-MT-OS peaking during the early afternoon samples but with an enhanced signal at night. There was also a strong correlation between these two species (R^2 = 0.92) during the campaign. The 2-MG-OS showed a stronger correlation with particulate sulfate (R^2=0.52) than 2-MT-OS (R^2=0.44), and there was also a weak anti-correlation with photochemical age (R^2=0.28). A strong correlation was also observed for 2-MG-OS with [O_3][pSO4] (R^2=0.69), as shown in Figure 5, highlighting that formation is dependent on both photochemistry and sulfate aerosol availability.

3.4.3 Other isoprene-related OSs and NOSs

24 additional OSs species, with molecular formulae consistent with iSOA tracers seen in chamber experiments, were also observed in Beijing as shown in Table 1. For C_5 compounds, the most abundant species were $C_5H_{10}SO_6$ and $C_5H_{10}SO_5$, with mean concentrations of 28.7 ng m^{-3} and 26.5 ng m^{-3}, respectively. The identity of the OS at *m/z* 182 ($C_5H_{10}SO_5$) is currently unknown and the product ion MS provides little additional information other than sulfate-related fragment ions at *m/z* 97 and *m/z* 80. The OS at m/z 198 ($C_5H_{10}SO_6$) was identified as an IEPOX-related OS in chamber experiments by Nestorowicz *et al.* (2018), but at relatively low concentrations compared to the 2-MT-OS (1-4 %). This is very different to the observed ratio is Beijing, where the $C_5H_{10}SO_6$ average concentration was more than double that of 2-MT-OS, as shown in Figure 4c. This compound showed a strong correlation with 2-MT-OS (R^2 = 0.77) but it is currently unclear why this compound is the most abundant C_5 species. The molecular weight of this species is 18 Da (-H_2O) lower than 2-MT-OS, which may indicate it is a dehydration product enhanced under acidic aerosol conditions. In addition, this species may also be enhanced if it is formed from additional VOC precursors.

Potential low-NO iSOA tracers, seen in chamber experiments, correlated strongly with the 2-MT-OS including unresolved isomers of cyclic hemiacetals [$C_5H_{10}SO_7$ (R^2=0.92)], and lactones [$C_5H_8SO_7$ (R^2=0.83)] (Spolnik et al., 2018). These compounds were similar in concentration to the 2-MT-OS, with

https://doi.org/10.5194/acp-2019-929
Preprint. Discussion started: 23 October 2019

Atmospheric Chemistry and Physics Discussions

the lactones at MW 212 having a mean concentration of 14 ng m^{-3} and the cyclic hemiacetals at MW 214 a mean of 10.6 ng m^{-3}. These compounds were also observed to be the dominant type of isoprene-derived OSs in Atlanta, Georgia, although they had concentrations a factor of ~15 times lower than the observed 2-MT-OS. (Hettiyadura et al., 2019)

Additional small OS compounds, previously identified during high-NO chamber experiments, were also observed in Beijing, including in order of decreasing concentration, glycolic acid sulfate ($C_2H_4SO_6$, mean = 38.4 ng m^{-3}), hydroxyacetone sulfate ($C_3H_6SO_5$, mean = 20.5 ng m^{-3}) and lactic acid sulfate ($C_3H_6SO_6$, mean = 14.5 ng m^{-3}) (Surratt et al., 2007; Surratt et al., 2008). These concentrations are in line with measurements made in other urban locations (Rattanavaraha et al., 2016; Huang et al., 2018; Hettiyadura et al., 2018). While all three C_2-C_3-OS compounds had strong correlations with the other iSOA OS tracers (R^2 = 0.6-0.94), the relative strength of isoprene versus other VOC precursors, such as aromatics, cannot be determined. As such, they cannot be definitively assigned as iSOA tracers, and are therefore included in the potential iSOA portion of Figure 6. The sum of the C_2 and C_3 OSs had an average concentration of 73 ng m^{-3}, with a range of 2.0-831 ng m^{-3}.

In addition, 9 NOS species related to isoprene were identified as shown in Table 1 (Ng et al., 2008; Rollins et al., 2009). Some of the NOS observed peaked in the daytime and some were enhanced at night. In total they had a mean concentration of 24 ng m^{-3} during the campaign. The sources and formation of these species will be discussed in a separate publication.

3.5 Contribution of Isoprene SOA in Beijing

In order to estimate the total amount of isoprene-derived OSs and NOSs, labelled here as iSOA, 13 species were chosen that could be confidently identified as being predominately from isoprene (2-MT-OS, 2-MG-OS, $C_5H_{10}SO_7$, $C_5H_8SO_7$, $C_5H_{11}NSO_9$, $C_5H_9NSO_{10}$, $C_5H_9N_2SO_{11}$, $C_5H_8N_3SO_{13}$). Although there were a number of other compounds with formula similar to iSOA tracers, their trends compared to previous studies and potential for alternative sources made a confident assignment of VOC precursor difficult. Therefore, the estimated contribution of iSOA to the observed total particulate mass determined here should be taken as a lower limit. Figure 6 shows the time series of the iSOA observed in Beijing. The average concentration was 82.5 ng m^{-3} during the campaign, ranging from 718 ng m^{-3} on the 19/05/2017 (11:38 – 14:30) to 1.9 ng m^{-3} on the 02/06/2017 (14:36-17:28). The contribution of iSOA to the OOA factors measured by the AMS was obtained by assuming all OSs and NOSs species fragment in the ion source to lose the sulfate and nitrate groups. Across the whole measurement period, the iSOA tracers represented only a small fraction of the total OOA measured by AMS (0.62% of ∑[OOA1-3]). However, towards the end of the measurement period, this increased up to a maximum of 3 % on the 17/06/2017 (13:32-14:23).

Additional iSOA tracers containing only CHO, including 2-methyltetrols, 2-methyglyceric acid and C_5-alkene triols, were measured in separate 24-hour filter samples, with the commonly used derivatization GC-MS method (Claeys et al., 2004; Wang et al., 2005.). The average ratio of the 2-methyltetrols to its

https://doi.org/10.5194/acp-2019-929
Preprint. Discussion started: 23 October 2019

Atmospheric Chemistry and Physics Discussions

corresponding OS (2-MT:2-MT-OS) was 1.4, indicating extensive heterogeneous conversion of isoprene oxidation products within the particles. The observed ratio is slightly larger than those measured in the SE US (~0.37-0.96 as shown in Table 2) but much lower than that measured in the Pearl River Delta region (~40,) where the 2-methyltetrols dominated. In contrast, the average ratio of the high-NO iSOA tracer, 2-MG and its corresponding organosulfate (2-MG:2-MG-OS) observed in Beijing was 0.33, indicating more extensive transformation to heterogeneous products. This ratio may also reflect the more volatile nature of 2-MG compared to 2-MT. Overall, the combined concentrations of these isoprene CHO compounds were generally low (mean 25 ng m^{-3}, max 69 ng m^{-3}) in comparison to the heterogeneous iSOA compounds (i.e., isoprene-derived OSs and NOSs) targeted in this work. In addition, the concentrations of these CHO species may be overestimated based on recent studies demonstrating that thermal decomposition leads to these products being detected by GC-MS and FIGAERO-CIMS methods (D'Ambro et al., 2019), and so the conversion to heterogeneous products (i.e., OSs and NOSs) may in fact be larger (2MT:2MT-OS = 0.5-0.91 using the overestimates of 160-288 % observed in Cui et al., (2018)).

The study presented here shows for the first time that OS species derived from isoprene oxidation can make a significant contribution to oxidised organic aerosol in Beijing in summer. There is significant anthropogenic control, from both NO_x and sulfate aerosols, on the products and concentrations of iSOA in Beijing. The majority of the OS species showed a strong correlation towards the product of $[O_3][pSO_4]$, highlighting the role of both photochemistry and the availability of particulate sulfate for heterogeneous reactions. When the observed concentrations of all the OS and NOS species measured in this study, including the additional 19 compounds not confidently assigned to iSOA, are combined they contribute on average 2.2 % to the total OOA (∑[OOA1-3]), increasing to a maximum of 10.5 %, indicating extensive heterogeneous conversion of VOC oxidation products in Beijing in summer.

Author contributions

DB analysed the aerosol samples and quantified iSOA tracers. WD and KP developed the UPLC-MS method. JRH, RD and MS provided the VOC measurements. FS and JL collected the NO, NO_2 and O_3 data. TB, AM, SW, AB, CJP, HC collected and analysed the CIMS data. LW, DH and ES provided the OH and HO_2 data and BO provided the NO_3 measurements. TC, JDS and WD carried out the offline HILIC analysis. DL, ZS and RH provided the GC-MS iSOA data. YS and WX carried out the AMS measurements and PMF analysis. ACL and RH lead the APHH projects. DB, ARR and JFH wrote the manuscript with input and discussion with all co-authors.

Competing interests

The authors declare that they have no conflict of interest.

Acknowledgements

This project was funded by the Natural Environment Research Council, the Newton Fund and Medical Research Council in the UK, and the National Natural Science Foundation of China (NE/N007190/1,

https://doi.org/10.5194/acp-2019-929
Preprint. Discussion started: 23 October 2019

NE/N006917/1). We acknowledge the support from Pingqing Fu, Zifa Wang, Jie Li and Yele Sun from IAP for hosting the APHH-Beijing campaign at IAP. We thank Tuan Vu and Bill Bloss from the University of Birmingham, Siyao Yue, Liangfang Wei, Hong Ren, Qiaorong Xie, Wanyu Zhao, Linjie Li, Ping Li, Shengjie Hou, Qingqing Wang from IAP, Kebin He and Xiaoting Cheng from Tsinghua University, and James Allan from the University of Manchester for providing logistic and scientific support for the field campaigns. Daniel Bryant, Freya Squires, William Dixon and Eloise Slater acknowledge NERC SPHERES PhD studentships. Marvin Shaw acknowledges SYFT Technologies for his fellowship grants and scientific support. The Orbitrap-MS was funded by a Natural Environment Research Council strategic capital grant, CC090. Jason Surratt and Tianqu Cui acknowledge support from the United States National Science Foundation (NSF) under Atmospheric and Geospace (AGS) Grant 1703535 as well as thank Avram Gold and Zhenfa Zhang from the University of North Carolina for providing the 2-MT-OS and 2-MG-OS standards.

References

Atkinson, R., Baulch, D. L., Cox, R. A., Crowley, J. N., Hampson, R. F., Hynes, R. G., Jenkin, M. E., Rossi, M. J., Troe, J., and IUPAC Subcommittee: Evaluated kinetic and photochemical data for atmospheric chemistry: Volume II – gas phase reactions of organic species, Atmos. Chem. Phys., 6, 3625-4055, https://doi.org/10.5194/acp-6-3625-2006, 2006.

Bannan, T. J., Booth, A. M., Bacak, A., Muller, J. B., Leather, K. E., Le Breton, M., Jones, B., Young, D., Coe, H., Allan, J., Visser, S., Slowik, J. G., Furger, M., Prévôt, A. S. H., Lee, J., Dunmore, R. E., Hopkins, J. R., Hamilton, J. F., Lewis, A. C., Whalley, L. K., Sharp. T., Stone, D., Heard, D. E., Fleming. Z. L., Leigh, R., Shallcross, D. E., and Percival C. J.: The first UK measurements of nitryl chloride using a chemical ionization mass spectrometer in central London in the summer of 2012, and an investigation of the role of Cl atom oxidation, J. Geophys. Res., 120, 5638-5657, https://doi.org/10.1002/2014JD022629, 2015.

Bannan, T. J., Le Breton, M., Priestley, M., Worrall, S. D., Bacak, A., Marsden, N. A., Mehra, A., Hammes, J., Hallquist, M., Alfarra, M. R., Krieger, U, K., Reid, J. P., Jayne, J., Robinson, W., McFiggins, G., Coe, H., Percival, C. J., and Topping, D.: A method for extracting calibrated volatility information from the FIGAERO-HR-ToF-CIMS and its experimental application, Atmos. Meas. Tech., 12, 1429-1439, https://doi.org/10.5194/amt-12-1429-2019, 2019.

Beelen, R., Raaschou-Nielsen, O., Stafoggia, M., Andersen, Z. J., Weinmayr, G., Hoffmann, B., Wolf, K., Samoli, E., Fischer, P., Nieuwenhuijsen, M., Vineis, P., Xun, W. W., Katsouyanni, K., Dimakopoulou, K., Oudin, A., Forsberg, B., Modig, L., Havulinna, A. S., Lanki, T., Turunen, A., Oftedal, B., Nystad, W., Nafstad, P., De Faire, U., Pedersen, N. L., Ostenson, C. G., Fratiglioni, L., Penell, J., Korek, M., Pershagen, G., Eriksen, K. T., Overvad, K., Ellermann, T., Eeftens, M., Peeters, P. H., Meliefste, K., Wang, M., Bueno-de- Mesquita, B., Sugiri, D., Kramer, U., Heinrich, J., de Hoogh, K., Key, T., Peters, A., Hampel, R., Concin, H., Nagel, G., Ineichen, A., Schaffner, E., Probst-Hensch, N., Kunzli, N., Schindler, C., Schikowski, T., Adam, M., Phuleria, H., Vilier, A., Clavel-Chapelon, F., Declercq, C., Grioni, S., Krogh, V., Tsai, M. Y., Ricceri, F., Sacerdote, C., Galassi, C., Migliore, E., Ranzi, A., Cesaroni, G., Badaloni, C., Forastiere, F., Tamayo, I., Amiano, P., Dorronsoro, M., Katsoulis, M., Trichopoulou, A., Brunekreef, B., and Hoek, G.: Effects of long-term exposure to air pollution on natural-cause mortality: an analysis of 22 European cohorts within the multicentre ESCAPE project, Lancet., 383, 785-795, https://doi.org/10.1016/S0140-6736(13)62158-3, 2014.

Budisulistiorini, S. H., Canagaratna, M. R., Croteau, P. L., Marth, W. J., Baumann, K., Edgerton, E. S., Shaw, S. L., Knipping, E. M., Worsnop, D. R., Jayne, J. T., Gold, A., Surratt, J. D.: Real-time continuous characterization of secondary organic aerosol derived from isoprene epoxydiols in downtown Atlanta, Georgia, using aerodyne aerosol chemical speciation monitor, Environ. Sci. Technol., 47, 5686-5694, https://doi.org/10.1021/es400023n, 2013.

https://doi.org/10.5194/acp-2019-929
Preprint. Discussion started: 23 October 2019

Atmospheric Chemistry and Physics Discussions

Budisulistiorini, S. H., Baumann, K., Edgerton, E. S., Bairai, S. T., Mueller, S., Shaw, S. L., Knipping, E. M., Gold, A., and Surratt, J. D.: Seasonal characterization of submicron aerosol chemical composition and organic aerosol sources in the southeastern United States: Atlanta, Georgia,and Look Rock, Tennessee, Atmos. Chem. Phys., 16, 5171–5189, https://doi.org/10.5194/acp-16-5171-2016, 2016.

Carlton, A. G., Wiedinmyer, C., Kroll, J. H., and Kroll, J. H.: A review of Secondary organic aerosol (SOA) formation from isoprene, Atmos. Chem. Phys., 9, 4987-5005, https://doi.org/10.5194/acp-9-4987-2009, 2009.

Chan, C. K., Yao, X.: Air pollution in mega cities in China, Atmos. Environ., 42, 1−42, https://doi.org/10.1016/j.atmosenv.2007.09.003, 2008.

Chan, M. N., Surratt, J. D., Claeys, M., Edgerton, E. S., Tanner, R. L., Shaw, S. L., Zheng, M., Knipping, E. M., Eddingsaas, N. C., Wennberg, P. O., and Seinfeld, J. H.: Characterization and quantification of isoprene-derived epoxydiols in ambient aerosol in the southeastern united states, Environ. Sci. Technol., 44, 4590-4596, https://doi.org/10.1021/es100596b, 2010.

Chen, Q., Farmer, D. K., Rizzo, L. V., Pauliquevis, T., Kuwata, M., Karl, T. G., Guenther, A., Allan, J. D., Coe, H., Andreae, M. O., Pöschl, U., Jimenex, J. L., Artaxo, P., and Martin, S. T.: Submicron particle mass concentrations and sources in the Amazonian wet season (AMAZE-08), Atmos. Chem. Phys., 15, 3687-3701, https://doi.org/10.5194/acp-15-3687-2015, 2015.

Chhabra, P. S., Flagan, R. C., and Seinfeld, J. H.: Elemental analysis of chamber organic aerosol using an aerodyne high-resolution aerosol mass spectrometer, Atmos. Chem. Phys, 10, 4111-4131, https://doi.org/acp-10-4111-2010, 2010.

Claeys, M., Graham, B., Vas, G., Wang, W., Vermeylen, R., Pashynska, Cafmeyer, J., Guyon, P., Andreae, M. O., Artaxo, P., and Maenhaut, W.: Formation of Secondary Organic Aerosols Through Photooxidation of Isoprene, Science., 303, 1173-1176, https://doi.org/10.1126/science.1092805, 2004.

Clark, C. H., Kacarab, M., Nakao, S., Asa-Awuku, A., Sato, K., and Cocker, D. R.: Temperature Effects on Secondary Organic Aerosol (SOA) from the Dark Ozonolysis and Photo-Oxidation of Isoprene, Environ. Sci. Technol., https://doi.org/10.1021/acs.est.5b05524, 2016.

Cui, T., Zeng, Z., dos Santos, E. O., Zhang, Z., Chen, Y., Zhang, Y., Rose, C. A., Budisulisyiorini, S. H., Collins, L. B., Bodnar, W. M., de Souza, R. A. F., Martin, S. T., Machado, C. M. D., Turpin, B. J., Gold, A., Ault, A. P., and Surratt, J. D: Development of hydrophilic interaction liquid chromatography (HILIC) method for the chemical characterization of water-soluble isoprene epoxydiol (IEPOX)-derived secondary organic aerosol, Environ. Sci., 20, 1524-1536, https://doi.org/10.1039/c8em00308d, 2018.

D'Ambro, E. L., Schobesberger, S., Gaston, C. J., Lopez-Hilfiker, F. D., Lee, B. H., Liu, J., Zelenyuk, A., Bell, D., Cappa, C. D., Helgestad, T., Li, Z., Guenther, A., Wang, J., Wise, M., Caylor, R., Surratt, J. D., Riedel, T., Hyttinen, N., Salo, V. -T., Hasan, G., Kurtén, T., Shilling, J. E., and Thornton, J. A: Atmos. Chem. Phys. Discuss., https://doi.org/10.5194/acp-2019-271, in review, 2019.

Ding, X., He, Q. -F., Shen, R. -Q., Yu, Q. -Q., and Wang, X. -M.: Spatial distributions of secondary organic aerosols from isoprene, monoterpenes, β-caryophyllene, and aromatics over China during summer, J. Geophys. Res., 119, 11877-11891, http://doi.org/10.1002/2014JD021748, 2014.

Dockery, D. W., Pope, C. A., Xu, X. P., Spengler, J. D., Ware, J. H., Fay, M. E., Ferris, B. G., Speizer, F. E.: An Association between Air- Pollution and Mortality in 6 United-States Cities, N. Engl. J. Med., 329, 1753−1759, https://doi.org/10.1056/NEJM199312093292401, 1993.

Dommen, J., Metzger, A., Duplissy, J., Kalberer, M., Alfarra, M. R., Gascho, A., Weingartner, E., Prevot, A. S. H., Vergeggen and B., Baltensperger.: Geo. Res. Lett., 33, L13805, https://doi.org/10.1029/2006GL026523, 2016.

https://doi.org/10.5194/acp-2019-929
Preprint. Discussion started: 23 October 2019

Atmospheric Chemistry and Physics Discussions

Edney, E. O., Kleindienst, T. E., Jaoui, M., Lewandowksi, M., Offenberg, J. H., Wang, W., and Claeys, M.: Formation of 2-methyl tetrols and 2-methylglyceric acid in secondary organic aerosol from laboratory irradiated isoprene/NO_X/SO_2/air mixtures and their detection in ambient $PM_{2.5}$ samples collected in the eastern United States, Atmospheric. Environ., 39, 5281-5289, https://doi.org/10.1016/j/atmosenv.2005.05.031, 2005.

Fu, P., Kawamura, K., Kanaya, Y., and Wang, Z.: Contributions of biogenic volatile organic compounds to the formation of secondary organic aerosols over Mt. Tai, Central East China, Atmos. Environ., 44, 4817-4826., https://doi.org/10.1016/j.atmosenv.2010.08.040, 2010.

Gaston, C. J., Riedel, T. P., Zhang, Z., Gold, A., Surratt, J. D., and Thornton, J. A.: Reactive uptake of an isoprene-derived epoxydiol to submicron aerosol particles, Environ. Sci. Technol., 48, 11178-11186, https://doi.org/10.1021/es5034266, 2014.

Glasius, M., Bering, M. S., Yee, L. D., De Sá, S. S., Isaacman-VanWertz, G., Wernis, R. A., Barbosa, H. M. J., Alexander, M. L., Palm, B. B., Hu, W., Campuzano-Jost, P., Day, D. A., Jimenez, J. L., Shrivastava, M., Martin, S. T., and Goldstein, A. H.: Organosulfates in aerosols downwind of an urban region in central Amazon, Environ. Sci.: Process. Impact., 20, 1546-1558., https://doi.org/10.1039/c8em00413g, 2018.

Hamilton, J. F., Lewis, A. C., Carey, T. J., and Wenger, J. C.: Characterization of Polar Compounds and Oligomers in Secondary Organic Aerosol Using Liquid Chromatography Coupled to Mass Spectrometry, Anal. Chem., 80, 474-480, https://doi.org/10.1021/ac701852t, 2008.

He, Q. -F., Ding, X., Fu, X. -X., Zhang, Y. -Q., Wang, J. -Q., Liu, Y. -X., Tang, M. -J., Wang, X. -M., and Rudich, Y.: Secondary Organic Aerosol Formation From Isoprene Epoxides in the Pearl River Delta, South China: IEPOX- and HMML- Derived Tracers, J. Geophys. Res. Atmos., 123, 6999-7012, https://doi.org/10.1029/2017JD028242, 2018.

Hettiyadura, A. P. S., Al-Naiema, I. M., Hughes, D. D., Fang, T., and Stone, E. A.: Organosulfates in Atlanta, Georgia: anthropogenic influences on biogenic secondary organic aerosol formation, Atmos. Chem. Phys., 19, 3191-3206, https://doi.org/10.5194/acp-19-3191-2019, 2019.

Hettiyadura, A. P. S., Xu, L., Jayarathne, T., Skog, K., Guo, H., Weber, R. J., Nenes, A., Keutsch, F. N., Ng, N. L., and Stone, E. A.: Source apportionments of organic in Centreville, AL using organosulaftes in organic tracer-based positive matrix factorization, Atm. Environ., 186, 74-88, https://doi.org/10.1016/j.atmosenv.2018.05.007, 2018.

Hopkins, J. R., Jones, C. E., and Lewis, A. C.: A dual channel gas chromatograph for atmospheric anlysis of volatile organic compounds including oxygenated and monoterpene compounds, J. Environ. Monit., 13, 2268-2276, https://doi.org/10.1039/clem10050e, 2011.

Hu, J., Huang, L., Chen, M., Liao, H., Zhang, H., Wang, S., Zhang, Q., and Ying, Q.: Premature Mortality Attributable to Particulate Matter in China: Source Contributions and Responses to Reductions, Environ. Sci. Technol., 52, 9950-9959, https://doi.org/10.1021/acs.est.7b03193, 2017a.

Hu, J., Li, Xun., Huang, L., Ying, Q., Zhang, Q., Zhao, B., Wang, S., and Zhang, H.: Ensemble prediction of air quality using the WRF/CMAQ model system for health effect studies in China, Atmos. Chem. Phys., 17, 13103-13118, https://doi.org/10.5194/acp-17-13103-2017, 2017b.

Hu, J., Wang, Y., Ying, Q., Zhang, H.: Spatial and temporal variability of PM2.5 and PM10 over the North China Plain and the Yangtze River Delta, China, Atmos. Environ., 95, 598−609, https://doi.org/10.1016/j.atmosenv.2014.07.019, 2014.

Hu, W. W., Campuzano-Jost, P., Palm, B. B., Day, D. A., Ortega, A. M., Hayes, P. L., Krechmer, J. E., Chen, Q., Kuwata, M., Liu, Y. J., De Sá, S. S., McKinney, K., Martin, S. T., Hu, M., Budisulistiorini, S. H., Riva, M., Surratt, J. D., St. Clair, J. M., Isaacman-Van Wertz, G., Yee, L. D., Goldstein, A. H., Carbon, S., Brito, J., Artaxo, P., De Gouw, J. A., Koss, A., Wisthaler, A., Mikoviny, T., Karl, T., Kaser, L., Jud, W., Hansel, A., Doucherty, K, S., Alexander, M. L., Robinson, N. H., Coe, H., Allan, J. D., Canagaratna, M. R., Paulot, F., and Jimenez, J. L.: Characterization of a real-time tracer for

https://doi.org/10.5194/acp-2019-929
Preprint. Discussion started: 23 October 2019

Atmospheric Chemistry and Physics Discussions

isoprene epoxydiols-derived secondary organic aerosol (IEPOX-SOA) from aerosol mass spectrometer measurements, Atmos. Chem. Phys., 15, 11807-11833, https://doi.org/10.5194/acp-15-11807-2015, 2015.

Hu, W. W., Campuzano-Jost, P., Palm. B. B., Day, D. A., Ortega, A. M., Hayes, P. L., Krechmer, J. E., Chen, Q., Kuwata, M., Liu, Y. J., De Sá, S. S., McKinney, K., Martin, S. T., Hu, M., Budisulistiorini, S. H., Riva, M., Surratt, J. D., St. Clair, J. M., Isaacamn-Van Wertz, G., Yee, L. D., Goldstein, A. H., Carbone, S., Brito, J., Artaxo, P., De Gouw, J. A., Koss, A., Wisthaler, A., Milkoviny, T., Karl, T., Kaser, L., Jud, W., Hansel, A., Docherty, K. S., Alexander, M. L., Robinson, N. H., Coe, H., Allan, J. D., Canagaratna, M. R., Paulot, F., and Jimenez, J. L.: characterization of a real-time tracer for isoprene epoxydiols-derived secondary organic aerosol (IEPOX-SOA) from aerosol mass spectrometer measurements, Atmos. Chem. Phys., 15, 11807-11833, https://doi.org/10.5194/acp-15-11807-2015, 2015.

Hu, W., Hu, M., Hu, W., Jimenez, J. L., Yuan, B., Chen, W., Wang, M., Wu, Y., Chen, C., Wang, Z., Peng, J., Zeng, L., and Shao, M.: Chemical Composition, sources, and aging process of submicron aerosols in Beijing: Contrast between summer and winter, J. Geophys. Res. Atmos., 121, 1955-1977, https://doi.org/10.1002/2015JD024020, 2016.

Huang, R. -J., Cao, J., Chen, Y., Yang, L., Shen, J., You, Q., Wang, K., Lin, C., Xu, W., Gao, B., Li, Y., Chen, Q., Hoffmann, T., O'Dowd, C. D., Bilde, M., and Glasius.: Organosulfates in atmospheric aerosol: Synthesis and quantitative analysis of PM2.5 from Xi'an, northwestern China, Atmos. Meas. Tech., 11, 3447-3456, https://doi.org/10.5194/amt-11-3447-2018, 2018.

Jacobs, M. I., Burke, W. J., and Elrod, M. J.: Kinetics of the reactions of isoprene-derived hydroxynitrates: gas phase epoxide formation and solution phase hydrolysis, Atmos. Chem. Phys., 14, 8933-8946, https://doi.org/10.5194/acp-14-8933-2014, 2014.

Jerrett, M., Burnett, R. T., Pope, C. A., Ito, K., Thurston, G., Krewski, D., Shi, Y. L., Calle, E., Thun, M.: Long-Term Ozone Exposure and Mortality, N. Engl. J. Med., 2009, 360, 1085−1095, https://doi.org/10.1056/NEJMoa0803894, 2009.

Kleindienst, T. E., Edney, O. E., Lewandowski, M., Offenberg, and J. H., Jaoui, M.: Secondary organic carbon and aerosol yields from the irradiations of isoprene and α-pinene in the presence of NOx and SO2, Environ. Sci. Technol., 40, 3807-3812, https://doi.org/10.1021/es052446r, 2016.

Kleindienst, T. E., Jaoui, M., Lewandowski, M., Offenberg, J. H., Lewis, C. W., Bhave, P. V., and Edney, E. O.: Estimates of the contributions of biogenic and anthropogenic hydrocarbons to secondary organic aerosol at a southeastern US location, Atmos. Environ., 41, 8288-8300, http://doi.org/10.1016/j.atmosenv.2007.06.045, 2007.

Krechmer, J. E., Coggon, M. M., Massoli, P., Nguyen, T. B., Crounse, J. D., Hu, W., Day, D. A., Tyndall, G. S., Henze, D. K., Rivera-Rios, J. C., Nowak, J. B., Kimmel, J. R., Mauldin, R. L., Stark, H., Jayne, J. T., Sipilä, M., Junninen, H., St.Clair, J. M., Zhang, X., Feiner, P. A., Zhang, L., Miller, D. O., Brune, W. H., Keutsch, F. N., Wennberg, P. O., Seinfeld, J. H., Worsnop, D. R., Jimenez, J. L., and Canagaratna, M. R.: Formation of Low Volatility Organic Compounds and Secondary Organic Aerosol from Isoprene Hydroxyhydroperoxide Low-NO Oxidation, Environ. Sci. Technol., 49, 10330-10339, https://doi.org/10.1021/acs.est.5b02031, 2015.

Krechmer, J. E., Groessl, M., Zhang, X., Junninen, H., Massoli, P., Lambe, A. T., Kimmel, J. R., Cubison, M. J., Graf, S., Lin, Y. -H., Budisulistiorini, S. H., Zhang, H., Surratt, J. D., Knochenmuss, R., Jayne, J. T., Worsnop, D. R., Jimenez, J. -L., and Canagaratna, M. R.: Ion mobility spectrometry-mass spectrometry (IMS-MS) for on- and offline analysis of atmospheric gas and aerosol species, Atmos. Meas. Tech., 9, 3245-3262, https://doi.org/10.5194/amt-9-3245-2016, 2016.

Kroll, J. H., Ng, N. L., Murphy, S. M., Flagan, R. C., and Seinfeld, J. H.: Secondary organic aerosol formation from isoprene photooxidation, Environ. Sci. Technol., 40, 1869-1877, https://doi.org/10.1021/es0524301, 2016.

https://doi.org/10.5194/acp-2019-929
Preprint. Discussion started: 23 October 2019

Laurent, O., Hu, J. L., Li, L. F., Cockburn, M., Escobedo, L., Kleeman, M. J., Wu, J.: Sources and contents of air pollution affecting term low birth weight in Los Angeles County, California, 2001−2008, Environ. Res., 134, 488−495, https://doi.org/10.1016/j.envres.2014.05.003, 2014.

Le Breton, M., Wang, Y., Hallquist, A. M., Kant Pathak, R., Zheng, J., Yang, Y., Shang, D., Glasius, M., Bannan, T. J., Liu, Q., Chank, C. K., Percival, C. J., Zhu, W., Lou, S., Topping, D., Wang, Y., Yu, J., Lu, K., Guo, S., Hu, M., and Hallquist, M.: Online gas- and particle-phase measurements of organosulfates, orgnanosulfonates and nitrooxy organosulaftes in Beijing utilizing a FIGAERO ToF-CIMS, 18, 10355-10371, https://doi.org/10.5194/acp-18-10355-2018, 2018.

Lee, B. H., Lopez-Hilfiker, F. D., Mohr, C., Kurtén, T., Worsnop, D. R., and Thornton, J. A.: An iodide-adduct high-resolution time-of-flight chemical-ionization mass spectrometer: Application to atmospheric inorganic and organic compounds. Environmental science & technology, 48(11), 6309-6317, 2014

Lelieveld, J., Evans, J. S., Fnais, M., Giannadaki, D., Pozzer, A.: The contribution of outdoor air pollution sources to premature mortality on a global scale, Nature., 525, 367-371, https://doi.org/10.1038/nature15371, 2015.

Li, J., Wang, G., Wu, C., Cao, C., Ren, Y., Wang, J., Li, J., Cao, J., Zeng, L., and Zhu, T.: Characterization of isoprene-derived secondary organic aerosols at a rural site in North China Plain with implications for anthropogenic pollution effects, Sci. Rep., 8, 1-10, https://doi.org/10.1038/s41598-017-18983-7, 2018.

Lin, Y. -H., Zhang, H., Pye, H. O. T., Zhang, Z., Marth, W. J., Park, S., Arashiro, M., Cui, T., Budisulistiorini, S. H., Sexton, K. G., Vizuete, W., Xie, Y., Luecken, D. J., Piletic, I. R., Edney, E. O., Bartolotti, L. J., Gold, A., and Surratt, J. D.: Epoxide as a precursor to secondary organic aerosol formation from isoprene photooxidation in the presence of nitrogen oxides, PNAS, 110, 6718-6723, https://doi.org/10.1073/pnas.1221150110, 2013.

Lin, Y. -H., Zhang, Z., Docherty, K. S., Zhang, H., Budisulistiorini, S. H., Rubitschun, C. L., Shaw, S. L., Knipping, E. M., Edgerton, E. S., Kleindienst, T. E., Gold, A., and Surratt, J. D.: Isoprene epoxydiols as precursors to secondary organic aerosol formation: Acid-catalyzed reactive uptake studies with authentic standards, Environ. Sci. Technol., 46, 250-258, https://doi.org/10.1021/es202554c, 2012.

Lopez-Hilfiker, F. D., Mohr, C., Ehn, M., Rubach, F., Kleist, E., Wildt, J., Mentel, Th. F., Lutz, A., Hallquist, M., Worsnop, D., and Thornton, J. A.: A novel method for online analysis of gas and particle composition: description and evaluation of a Filter Inlet for Gases and Aerosols (FIGAERO), Atmos. Meas. Tech., 7, 983-1001,https://doi.org/10.5194/amt-7-983-2014, 2014.

Nestorowicz, K., Jaoui, M., Jan Rudzinski, K., Lewandowski, M., Kleindienst, T. E., Spólnik, G., Danikiewicz, W., and Szmigielski, R.: Chemical composition of isoprene SOA under acidic and non-acidic conditions: Effect of relative humidity, Atmos. Chem. Phys., 18, 18101-18121, https://doi.org/10.5194/acp-18-18101-2018, 2018.

Newland, M. Rainforest-like Atmospheric Chemistry in a Polluted Megacity, In Review, 2019.

Ng, N. L., Kroll, J. H., Keywood, M. D., Bahreini, R., Varutbangkul, V., Flagan, R. C., Seinfeld, J. H., Lee, A., and Goldstein, A. H.: Contribution of first-versus second-generation products to secondary organic aerosols formed in the oxidation of biogenic hydrocarbons, Environ. Sci. Technol., 40, 2283-2297, https://doi.org/10.1021/es052269u, 2006.

Ng, N. L., Kwan, A. J., Surratt, J. D., Chan, A. W. H., Chhabra, P. S., Sorooshian, A., Pye, H. O. T., Crounse, J. D., Wennberg, P. O., Flagan, R. C., Seinfeld, J. H.: Secondary organic aerosol (SOA) formation from reaction of isoprene with nitrate radicals (NO_3), Atmos. Chem. Phys., 8, 3163–3226, https://doi.org/10.5194/acp-8-4117-2008, 2008.

Nguyen, Q. T., Christensen, M. K., Cozzi, F., Zare, A., Hansen, A. M. K., Kristensen, K., Tulinius, T. E., Madsen, H. H., Christensen, J. H., Brandt, J., Massling, A., Nøjgaard, J. K., and Glasius, M.:

https://doi.org/10.5194/acp-2019-929
Preprint. Discussion started: 23 October 2019

Understanding the anthropogenic influence on formation of biogenic secondary organic aerosols in Denmark via analysis of organosulfates and related oxidation products, Atmos. Chem. Phys., 14, 8961-8981, https://doi.org/10.5194/acp-14-8961-2014, 2014.

Nguyen, T. B., Bates, K. H., Crounse, J. D., Schwantes, R. H., Zhang, X., Kjaergaard, H. G., Surratt, J. D., Lin, P., Laskin, A., Seinfeld, J. H., and Wennberg, P. O.: Mechanism of the hydroxyl radical oxidation of methacryloyl peroxynitrate (MPAN) and its pathway toward secondary organic aerosol formation in the atmosphere, Phys. Chem., 17, 17914-17926, https://doi.org/10.1039/c5cp02001h, 2015.

Nguyen, T. B., Coggon, M. M., Bates, K. H., Zhang, X., Schwantes, R. H., Schilling, K. A., Loza, C. L., Flagan, R. C., Wennberg, P. O., and Seinfeld, J. H.: Organic aerosol formation from the reactive uptake of isoprene epoxydiols (IEPOX) onto non-acidified inorganic seeds, Atmos. Chem. Phys., 14, 3497-3510, https://doi.org/10.5194/acp-14-3497-2014, 2014.

Nguyen, T. B., Roach, P. J., Laskin, J., Laskin, A., and Nizkorodov.: Effect of humidity on the composition of isoprene photooxidation secondary organic aerosol, Atmos. Chem. Phys., 11, 6931-6944, https://doi.org/10.5194/acp-11-6931-2011, 2011.

Ostro, B., Hu, J., Goldberg, D., Reynolds, P., Hertz, A., Bernstein, L., Kleeman, M. J.: Associations of Mortality with LongTerm Exposures to Fine and Ultrafine Particles, Species and Sources: Results from the California Teachers Study Cohort, Environ. Health Perspect., 123, 549−556, https://doi.org/10.1289/ehp.1408565, 2015.

Pandis, S. N., Paulson, S. E., Seinfeld, J. H., and Flagan, R. C.: Aerosol formation in the photooxidation of isoprene and β-pinene, Atmospheric. Environ. Part A. General Topics., 25, 997-1008, https://doi.org/ 10.1016/0960-1686(91)90141-S, 1991.

Paulot, F., Crounse, J. D., Kjaergaard, H. G., Kürten, A., Clair, J. M. S., Seinfeld, J. H., and Wennberg, P. O.: Unexpected epoxide formation in the gas-phase photooxidation of isoprene, Science, 325, 730-733, https://doi.org/10.1126/science.1172910, 2009.

Pope, C. A., Dockery, D. W.: Health effects of fine particulate air pollution: Lines that connect, J. Air Waste Manage. Assoc.,56, 709−742, https://doi.org/10.1080/10473289.2006.10464485, 2006.

Pope, C. A.: Review: Epidemiological basis for particulate air pollution health standards, Aerosol Sci. Technol., 32, 4−14, https://doi.org/10.1080/027868200303885, 2000.

Priestley, M., Le Breton, M., Bannan, T. J., Leather, K. E., Bacak, A., Reyes-Villegas, E., De Vocht., F., Shallcross, B. M. A., Brazier, T., Khan, M. A., Allan, J., Shallcross, D., E., Coe, H., Percival, C. J.: Observations of isocyanate, amide, nitrate and nitro compounds from an anthropogenic biomass burning event using a ToF-CIMS, Journal of Geophysical Research: Atmospheres, 123, 7687-7704, https://doi.org/10.1002/2017JD027316, 2018.

Rattanavaraha, W., Chu, K., Budisulistiorini, S. H., Riva, M., Lin, Y. -H., Edgerton, E. S., Baumann, K., Shaw, S. L., Guo, H., King, L., Weber, R. J., Neff, M. E., Stone, E. A., Offenberg, J. H., Zhang, Z., Gold, A., and Surratt, J. D.: Assessing the impact of anthropogenic pollution on isoprene-derived secondary organic aerosol formation in $PM_{2.5}$ collected from Birmingham, Alabama, ground site during the 2013 Southern Oxidant and Aerosol Study, Atmos. Chem. Phys., 16, 4897-4914, https://doi.org/10.5194/acp-16-4897-2016, 2016.

Rattanavaraha, W., Canagaratna, M. R., Budisulistiorini, S. H., Croteau, P. L., Baumann, K., Canonaco, F., Prevot, A. S. H., Edgerton, E. S., Zhang, Z., Jayne, J. T., Worsnop, D. R., Gold, A., Shaw, S. L., and Surratt, J. D, Atmos. Environ., 167, 389-402, https://doi.org/10.1016/j.atmosenv.2017.07.055, 2017.

Riva, M., Budisulistiorini, H., Zhang, Z., Gold, A., Surratt, J. D.:Chemical characterization of secondary organic constituents from isoprene ozonolysis in the presence of acidic aerosol, Atmos. Environ., 130, 5-13, https://doi.org/10.1016/j.atmosenv.2015.06.027, 2016a.

https://doi.org/10.5194/acp-2019-929
Preprint. Discussion started: 23 October 2019

Riva, M., Budisulistiorini, S. H., Chen, Y., Zhang, Z., D'Ambro, E. L., Zhang, X., Gold, A., Turpin, B. J., Thornton, J. A., canagaratna, M. R., and Surratt, J. D.: Chemical Characterization of Secondary Organic Aerosol from Oxidation of Isoprene Hydroxyhydroperoxides, Environ. Sci. Technol., 50, 9889-9899, https://doi.org/10.1021/acs.est.5b05524, 2016b.

Riva, M., Chen, Y., Zhang, Y., Lei, Z., Olson, N. E., Boyer, H. C., Narayan, S., Yee, L. D., Green, H. S., Cui, T., Zhang, Z., Baumann, K., Fort, M., Edgerton, E., Budisulistiorini, S. H., Rose, C. A., Riberiro, I. O., Oliveira, R. L., dos Santa, E. O., Machado, C. M. D., Szopa, S., Zhao, Y., Alves, E. G., de Sá, S. S., Hu, W., Knipping, E. M., Shaw, S. L., Duvoisin, S. Jr., de Souza, R. A. F., Palm, B. B., Jimenez, J. -L., Glasius, M., Goldstein, A. H., Pye, H. O. T., Gold, A., Turpin, B. J., Vizuete, W., Martin, S. T., Thornton, J. A., Dutcher, C. S., Ault, A. P., and Surratt, J. D.: Increasing Isoprene Epoxydiol-to-inorganic Sulfate Aerosol ratio results in Extensive Conversion of Inorganic Sulfate to Organosulfur Forms: Implications for Aerosol Physicochemical Properties, Environ. Sci. Technol., 53, 8682-8694, https://doi.org/10.1021/acs.est.9b01019, 2019.

Riva, M., Rantala, P., Krechmer, E. J., Peräkylä, O., Zhang, Y., Heikkinene, l., Garmash, O., Yan, C., Kulmala, M., Worsnop, D., and Ehn, M.: Evaluating the performance of five different chemical ionization techniques for detecting gaseous oxygenated organic species, Atmos. Meas. Tech., 12, 2403-2421, https://doi.org/10.5194/amt-12-2403-2019, 2019.

Robinson, N. H., Hamilton, J. F., Allan, J. D., Langford, B., Oram, D. E., Chen, Q., Docherty, K., Farmer, D. K., Jimenez, J. L., Ward, M. W., Hewitt, C. N., Barley, M. H., Jenkin, M. E., Rickard, A. R., Martin, S. T., McFiggans, G., and Coe, H.: Evidence for a significant proportion of secondary organic aerosol from isoprene above a maritime tropical forest, Atmos. Chem. Phys., 11, 1039-1050, https://doi.org/10.5194/acp-11-1039-2011, 2011.

Rollins, A. W., Kiendler-Scharr, A., Fry, J. L., Brauers, T., Brown, S. S., Dorn, H. -P., Dubé, W. P., Fuchs, H., Mensah, A., Mentel, T. F., Rohrer, F., Tillman, R., Wegener, R., Woolridge, P. J., and Cohen, R. C: Isoprene oxidation by nitrate radical: alkyl nitrate and secondary organic aerosol yields, Atmos. Chem. Phys., 9, 6685-6703, https://doi.org/10.5194/acp-9-6685-2009, 2009.

Schwantes, R. H., Charan, S. M., Bates, K. H., Huang, Y., Nguyen, T. B., Mai, H., Kong, W., Flagan, R. C., and Seinfeld, J. H.: Low-volatility compounds contribute significantly to isoprene secondary organic aerosol (SOA) under high-NO_X conditions, Atmos. Chem. Phys., 19, 7255-7278, https://doi.org/10.5194/acp-19-7255-2019, 2019.

Shi, Z., Vu, T., Kotthaus, S., Grimmond, S., Harrison, R. M., Yue, S., Zhu, T., Lee, J., Han, Y., Demuzere, M., Dunmore, R. E., Ren, L., Liu, D., Wang, Y., Wild, O., Allan, J., Barlow, J., Beddows, D., Bloss, W. J., Carruthers, D., Carslaw, D. C., Chatzidiakou, L., Crilley, L., Coe, H., Dai, T., Doherty, R., Duan, F., Fu, P., Ge, B., Ge, M., Guan, D., Hamilton, J. F., He, K., Heal, M., Heard, D., Hewitt, C. N., Hu, M., Ji, D., Jiang, X., Jones, R., Kalberer, M., Kelly, F. J., Kramer, L., Langford, B., Lin, C., Lewis, A. C., Li, J., Li, W., Liu, H., Loh, M., Lu, K., Mann, G., McFiggans, G., Miller, M., Mills, G., Monk, P., Nemitz, E., O'Connor, F., Ouyang, B., Palmer, P. I., Percival, C., Popoola, O., Reeves, C., Rickard, A. R., Shao, L., Shi, G., Spracklen, D., Stevenson, D., Sun, Y., Sun, Z., Tao, S., Tong, S., Wang, Q., Wang, W., Wang, X., Wang, Z., Whalley, L., Wu, X., Wu, Z., Xie, P., Yang, F., Zhang, Q., Zhang, Y., Zhang, Y., and Zheng, M.: Introduction to Special Issue – In-depth study of air pollution sources and processes within Beijing and its surrounding region(APHH-Beijing), Atmos.Chem.Phys., https://doi.org/10.5194/acp-2018-922, 2019.

Spolnik, G., Wach, P., Rudzinski, K. J., Skotak, K., Danikiewicz, W., and Szmigielski, R.: Improved UHPLC-MS/MS Methods for Analysis of Isoprene-Derived Organosulfates, Anal. Chem., 90, 3416-3423, https://doi.org/10.1021/acs.analchem.7b05060, 2018.

Sun, Y., Xu, W., Zhang, Q., Jiang, Q., Canonaco, F., Prévôt, A. S. H., Fu, P., Li, J., Jayne, J., Worsnop, D. R., and Wang, Z.: Source apportionment of organic aerosol from 2-year highly time resolved measurements by an aerosol chemical speciation monitor in Beijing, China, Atmos. Chem. Phys., 18, 8469-8489, https://doi.org/10.5194/acp-18-8469-2018, 2018.

Surratt, J. D., Chan, A. W. H., Eddingsaas, N. C., Chan, M., Loza, C. L., Kwan, A. J., Hersey, S. P., Flagan, R. C., Wennberg, P. O., and Seinfeld. J. H.: Reactive intermediates revealed in secondary

https://doi.org/10.5194/acp-2019-929
Preprint. Discussion started: 23 October 2019

organic aerosol formation from isoprene, PNAS., 107, 6640-6645, https://doi.org/10.1073/pnas.0911114107, 2010.

Surratt, J. D., Gómez-González, Y., Chan, A. W. H., Vermeylen, R., Shahgholi, M., Kleindienst, T. E., Edney, E. O., Offenberg, J. H., Lewandowski, M., Jaoui, M., Maenhaut, W., Claeys, M., Flagan, R. C., and Seinfeld, J. H.: Organosulfate formation in biogenic secondary organic aerosol, J. Phys. Chem. A., 112, 8345-8378, https://doi.org/10.1021/jp802310p, 2008.

Surratt, J. D., Kroll, J. H., Kleindienst, T. E., Edney, E. O., Claeys, M., Sorooshian, A., Ng, N. L., Offenberg, J. H., Lewandowski, M., Jaoui, M., Flagan, R. C., and Seinfeld, J. H.: Evidence for organosulfates in secondary organic aerosol, Environ. Sci. Technol., 41, 517-527, https://doi.org/10.1021/es062081q, 2007a.

Surratt, J. D., Lewandowski, M., Offenberg, J. H., Jaoui, M., Kleindienst, T. E., Edney, E. O., and Seinfeld, J. H.: Effect of acidity on secondary organic aerosol formation from isoprene, Environ. Sci. Technol., 41, 5363-5369, https://doi.org/10.1021/es0704176, 2007b.

Surratt, J. D., Murphy, S. M., Kroll, J. H., Ng, N. L., Hildebrandt, L., Sorooshian, A., Szmigielski, R., Vermeylen, R., Maenhaut, W., Claeys, M., Flagan, R. C., and Seinfeld, J. H.: Chemical composition of secondary organic aerosol formed from the photooxidation of isoprene, J. Phys. Chem. A., 110, 31, https://doi.org/10.1021/jp061734m, 2006.

Wang, Q., He, X., Huang, H. X. H., Griffith, S. M., Feng, Y., Zhang, T., Zhang, Q., Wu, D., and Yu, J. Z.: impact of Secondary Organic Aerosol Tracers on Tracer-Based Source Apportionment of Organic Carbon and $PM_{2.5}$: A Case Study in the Pearl River Delta, China, Earth. Space. Chem., 1, 562-571, https://doi.org/10.1021/acsearthspacechem.7b00088, 2017.

Wang, W., Kourtchev, I., Graham, B., Cafmeyer, J., Maenhaut, W., and Claeys, M.: Characterization of oxygenated derivatives of isoprene related to 2-methyltetrols in Amazonian aerosols using trimethylsilylation and gas chromatography/ion trap mass spectrometry, Rapid Commun. Mass Spectrom., 19, 2005, https://doi.org/10.1002/rcm.1940, 2005.

Wang, Y., Hu, M., Guo, S., Wang, Y., Zheng, J., Yang, Y., Zhu, W., Tang, R., Li, X., Liu, Y., Le Breton, M., Du, Z., Shang, D., Wu, Y., Wu, Z., Song, Y., Lou, S., Hallquist, M., and Yu, J.: The secondary formation of organosulfates under interactions between biogenic emissions and anthropogenic pollutants in summer in Beijing, Atmos. Chem. Phys., 18, 10693-10713, https://doi.org/10.5194/acp-18-10693-2018, 2018.

Wennberg, P. O., Bates, K. H., Crounse, J. D., Dodson, L. G., McVay, R. C., Mertens, L. A., Nguyen, T. B., Praske, E., Schwantes, R. H., Smarte, M. D., St Clair, J. M., Teng, A. P., Zhang, X., and Seinfeld, J. H.: Gas-Phase Reactions of Isoprene and Its Major Oxidation Products, Chem. Rev., 118, 3337-3390, http://doi.org/10.1021/acs.chemrev.7b00439, 2018.

Whalley, L. K., Stone, D., Dunmore, R., Hamilton, J., Hopkins, J. R., Lee, J. D., Lewis, A.C., Williams, P., Kleffmann, J., Laufs, S., Woodward-Massey, R., Heard, D. E.: Understanding in situ ozone production in the summertime through radical observations and modelling studies during the Clean air for London project (ClearfLo). Atmos. Chem. Phys., 18, 2547-2571, https://doi.org/10.5194/acp-18-2547-2018, 2018.

Woodward-Massey, R., Observations of radicals in the atmosphere: measurement validation and model comparisons, PhD Thesis, http://etheses.whiterose.ac.uk/22164/, 2018.

Xu, L., Kollman, M. S., Song, C., Shiling, J. E., and Ng, N. L.: Effects of NOx on the volatility of secondary organic aerosol from isoprene photooxidation, Environ. Sci. Tecnol., 48, 2253-2262, https://doi.org/10.1021/es404842g, 2014.

Zhang, H., Lin, Y, -H., Zhang, Z., Zhang, X., Shaw, S. L., Knipping, E. M., Weber, R. J., Gold, A., Kamens, R. M., and Surratt, J. D.: Secondary organic aerosol formation from methacrolein photooxidation: Roles of NO_X level, relative humidity and aerosol acidity, Environ. Chem., 9, 247-262, https://doi.org/10.1071/EN12004, 2012.

https://doi.org/10.5194/acp-2019-929
Preprint. Discussion started: 23 October 2019

Zhang, H., Surratt, J. D., Lin, Y. H., Bapat, J., and Kamens, R.M.: Effect of relative humidity on SOA formation from isoprene/NO photooxidation: Enhancement of 2-methylglyceric acid and its corresponding oligoesters under dry conditions, Atmos. Chem. Phys., 11, 6411-6424, https://doi.org/10.5194/acp-11-6411-2011, 2011.

Zhang, Q., Jimenez, J. L., Canagaratna, M. R., Ulbrich, I. M., Ng, N. L., Worsnop, D. R., and Sun, Y.: Understanding atmospheric organic aerosols via factor analysis of aerosol mass spectrometry: a review, Anal. Bioanal. Chem., 401, 3045-3067, https://doi.orh/10.1007/s00216-011-5355-y, 2011.

Zhang, Y., Chen, Y., Lambe, A. T., Olson, N. E., Lei, Z., Craig, R. L., Zhang, Z., Gold, A., Onasch, T. B., Jayne, J. T., Worsnop, D. R., Gaston, C. J., Thornton, J. A., Vizuete, W., Ault, A. P., and Surratt, J. D.: Effect of the Aerosol-Phase State on Secondary Organic Aerosol Formation from the Reactive Uptake of Isoprene-Derived Epoxydiols (IEPOX), Environ. Sci. Technol. Lett., 5, 167-174, https://doi.org/10.1021/acs.estlett.8b00044, 2018.

Zhang, Y., Ren, H., Sun, Y., Cao, F., Chang, Y., Liu, Shoudong, L., Lee, X., Agrios, K., Kawamura, K., Liu, D., Ren, L., Du, W., Wang, Z., Prévôt, A. S. H., Szidat, S., and Fu, P.: High Contribution of Nonfossil Sources to Submicrometer Organic Aerosols in Beijing, China, Environ. Sci. Technol., 51, 7842-7852, https://doi.org/10.1021/acs.est.7b01517, 2017.

Zhang, Y., Sun, J., Zhang, X., Shen, X., Wang, T., and Qin, M.: Seasonal characterization of components and size distributions for submicron aerosols in Beijing, Sci. China Earth Sci., 56, 890-900, https://doi.org/10.1007/s11430-012-45-15-z, 2013.

Zhang, Y., Tang, L., Sun, Y., Favez, O., Canonaco, F., Albinet, A., Couvidat, F., Liu, D., Jayne, J. T., Wang, Z., Croteau, P. L., Canagaratna, M. R., Zhou, H., Prévôt, A. S. H., and Worsnop, D. R.: Limited formation of isoprene epoxydiols-derived secondary organic aerosol under NO_X-rich environments in Eastern China, Geophys. Res. Lett., 44, 2035-2043, https://doi.org/10.1002/2016GL072368, 2017.

Zhou, W., Zhao, J., Ouyang, B., Mehra, A., Xu, W., Wang, Y., Bannan, T. J., Worrall, S. D., Priestley, M., Bacak, A., Chen, Q., Xie, C., Wang, Q., Wang, J., Du, W., Zhang, Y., Ge, X., Ye, P., Lee, J. D., Fu, P., Wang, Z., Worsnop, D., Jones, R., Percival, C. J., Coe, H., and Sun, Y.: Production of N_2O_5 and $ClNO_2$ in summer in urban Beijing, China, Atmos. Chem. Phys., 18, 11581-11597, https://doi.org/10.5194/acp-18-11581-2018, 2018.

https://doi.org/10.5194/acp-2019-929
Preprint. Discussion started: 23 October 2019

Atmospheric Chemistry and Physics Discussions

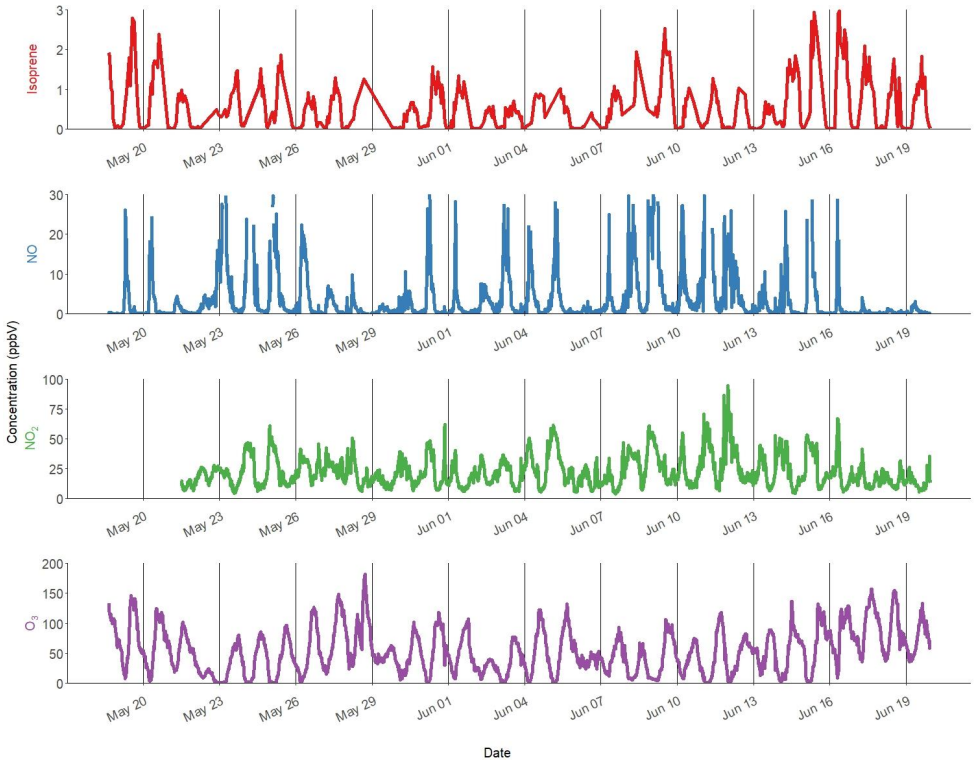

Figure 1. Time series of isoprene, nitric oxide (NO), nitrogen dioxide (NO_2), ozone (O_3).

https://doi.org/10.5194/acp-2019-929
Preprint. Discussion started: 23 October 2019

Atmospheric Chemistry and Physics Discussions

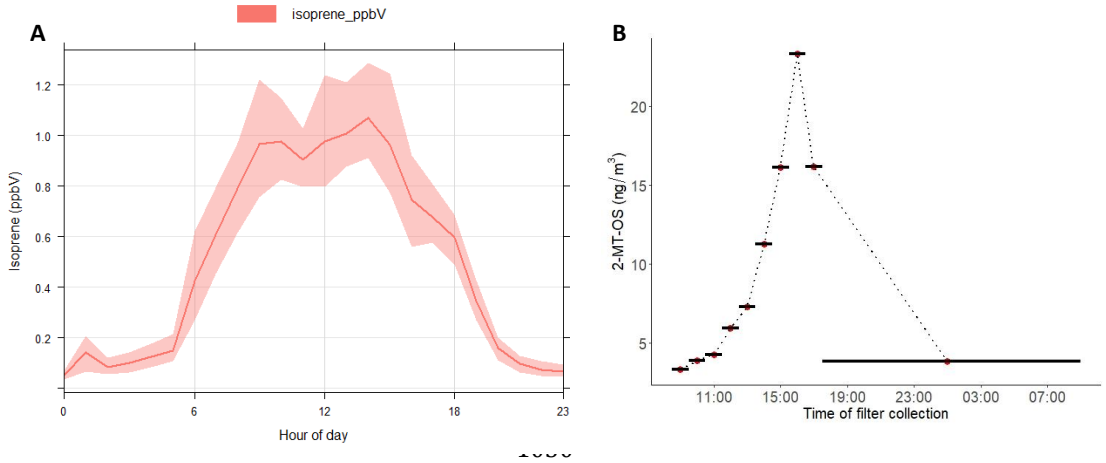

Figure 2. (A) Average diurnal profile of isoprene mixing ratio measured using DC-GC-FID. (B) Diurnal profile of 2-methyltetrol sulfate (2-MT-OS) in particulate matter ($PM_{2.5}$) collected on filters hourly over the 11th to 12th June 2017. Black lines indicate length of filter sampling period.

https://doi.org/10.5194/acp-2019-929
Preprint. Discussion started: 23 October 2019

Atmospheric Chemistry and Physics Discussions

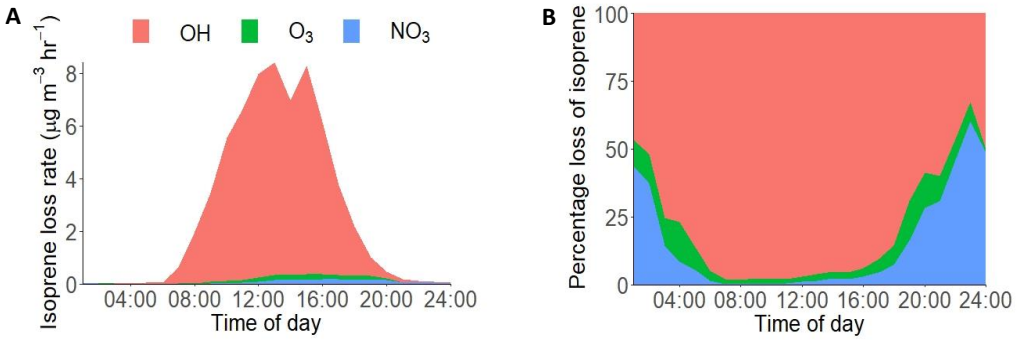

Figure 3. (A) Diurnal loss rate of isoprene calculated using measured average diurnal profiles of isoprene, OH, NO_3 and ozone. (B) Average diurnal of the percentage loss of isoprene from reactions with OH, O_3 and NO_3 radicals.The IUPAC rate constants used for the calculations are as follows, NO_3: $7x10^{-13}$, O_3:$1.27x10^{17}$, OH: $1x10^{10}$ (Atkinson et al., 2006).

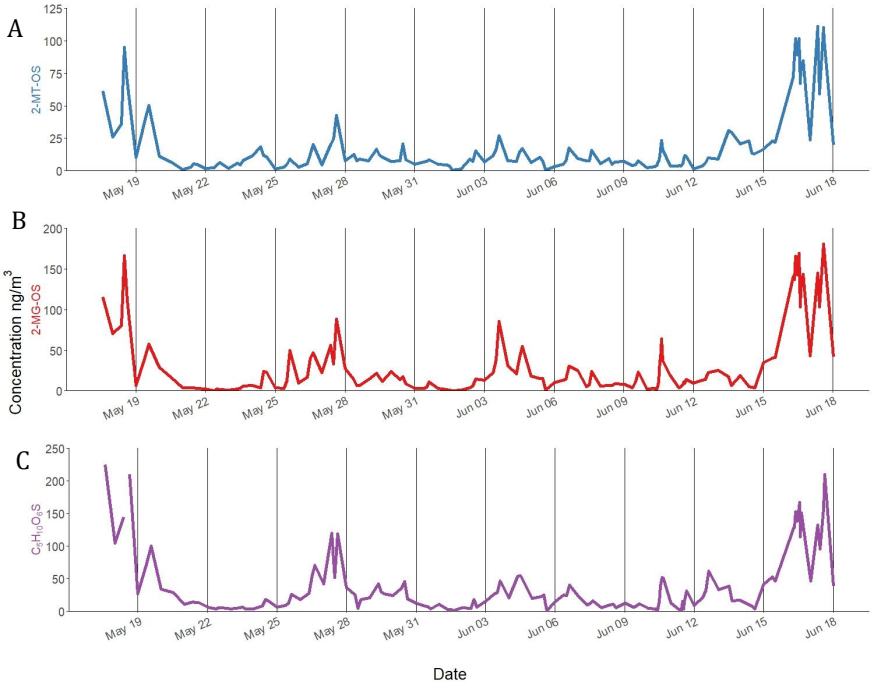

Figure 4. Time series of observed concentrations of iSOA tracers in Beijing during APHH. (A) 2-MT-OS ($C_5H_{12}O_7S$) (B) 2-MG-OS ($C_4H_8O_7S$ (C) $C_5H_{10}SO_6$. For ease of viewing a simple line is used to connect datapoints. It should be noted that the sampling time is not constant and details of the filter collection times are given in SI data. *(doi to be given on acceptance)*

https://doi.org/10.5194/acp-2019-929
Preprint. Discussion started: 23 October 2019

Atmospheric Chemistry and Physics Discussions

1110

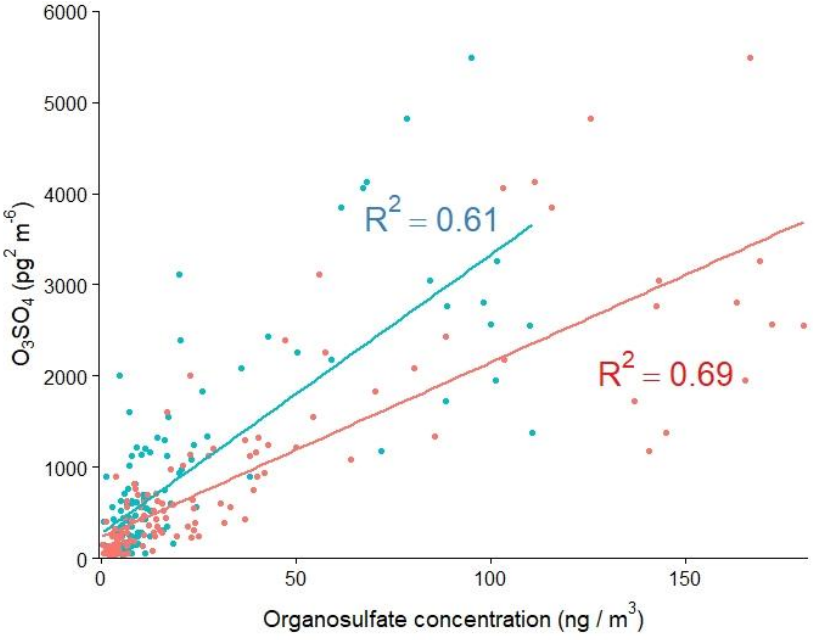

1115

Figure 5. Plot of 2-MT-OS ($C_5H_{12}O_7S$, blue) and 2-MG-OS ($C_4H_8O_7S$, red) concentrations versus [Ozone][SO_4]. The high time resolution data (O_3 and AMS SO_4^{2-}) has been averaged to the filter sampling time. The line was calculated using the stat_smooth function in the R package ggplot2, using the method "lm".

https://doi.org/10.5194/acp-2019-929
Preprint. Discussion started: 23 October 2019

Atmospheric Chemistry and Physics Discussions

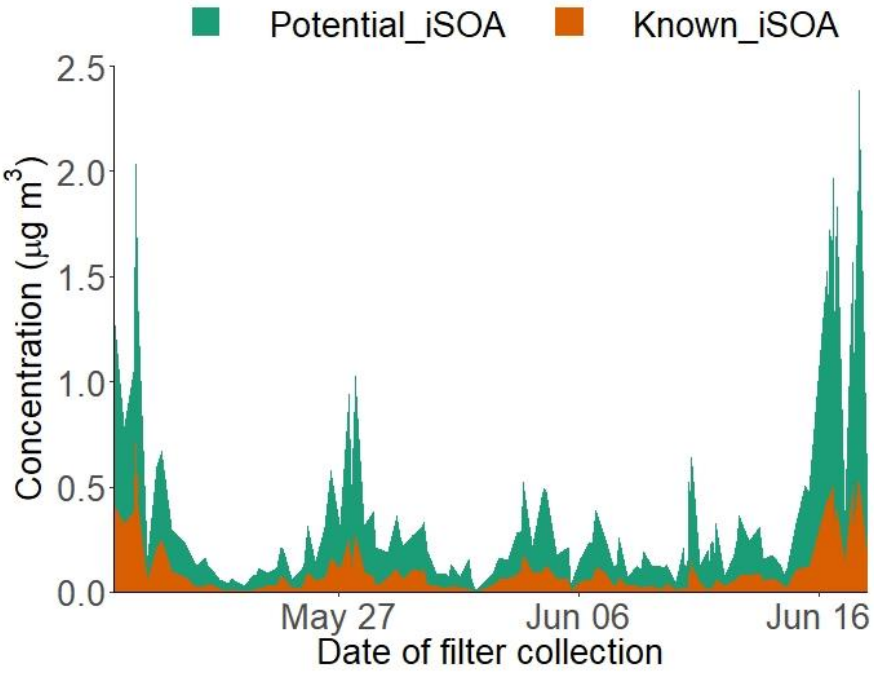

Figure 6. Time series of the total known isoprene SOA signal (2-MT-OS, 2-MG-OS, $C_5H_{10}SO_7$ (MW 214) $C_5H_8SO_7$ (MW 212) $C_5H_{11}NSO_9$ (MW 261), $C_5H_9NSO_{10}$ (MW 275) $C_5H_{10}O_{11}N_2S$ (MW 306), $C_5H_9O_{13}N_3S$ (MW 351) and the total signal from the other iSOA tracers quantified in this study.

https://doi.org/10.5194/acp-2019-929
Preprint. Discussion started: 23 October 2019

Atmospheric Chemistry and Physics Discussions

Table 1. Molecular formulas, negative ion masses, retention times (RT), time weighted means (ng m^{-3}) for the entire sampling period and original reference to where the tracer was found of each proposed iSOA tracer. BD = Below detection

Isoprene Tracer	$[M-H]^{-1}$	RT (min)	Time weighted mean (ng m^{-3})	Maximum (ng m^{-3})	Minimum (ng m^{-3})	Reference
$C_2H_4O_6S$	154.9656	0.73	38.4	366.1	BD	Surratt et al., 2008
$C_5H_{10}O_6S$	197.0125	0.79	28.7	336.2	0.25	Surratt et al., 2007
$C_5H_{10}O_5S$	181.0176	0.93	26.5	448.5	2.91	Nguyen et al., 2010
$C_4H_8O_6S$	182.9969	0.73	21.7	229.1	0.50	Riva et al., 2016
$C_4H_8O_7S$	198.9918	0.73	21.5	180.5	0.32	Surratt et al., 2007
$C_3H_6O_5S$	152.9863	0.73	20.5	327.9	0.98	Surratt et al., 2008
$C_3H_6O_6S$	168.9812	0.73	14.5	137.7	0.25	Surratt et al., 2008
$C_5H_8O_7S$	210.9918	0.73	14.0	136.4	0.27	Surratt et al., 2008
$C_5H_{11}O_9NS$	260.0082	0.86	12.6	154.1	0.10	Surratt et al., 2008
$C_5H_{12}O_7S$	215.0231	0.71	11.8	110.9	0.77	Surratt et al., 2008
$C_5H_{10}O_7S$	213.0075	0.73	10.6	104.7	0.38	Surratt et al., 2008
$C_5H_9O_{10}NS$	273.9874	0.94	9.17	53.8	BD	Nestorowicz et al., 2018
$C_4H_8O_5S$	167.0019	0.73	9.10	114.5	0.68	Surratt et al., 2007
$C_5H_8O_5S$	179.0020	0.85	6.59	144.2	0.43	Riva et al., 2016
$C_5H_{10}O_5S$	181.0176	1.24	4.90	36.3	1.21	Riva et al., 2016
$C_5H_{10}O_8S$	229.0024	0.75	4.59	40.9	BD	Nestorowicz et al., 2018
$C_5H_8O_9S$	242.9816	0.64	1.55	13.9	BD	Nestorowicz et al., 2018
$C_5H_{10}O_{11}N_2S$	304.9783	2.18	1.04	8.62	BD	Surratt et al., 2008
$C_{10}H_{20}O_8S$	299.0806	1.65	1.01	8.38	BD	Riva et al., 2016
$C_5H_{10}O_{11}N_2S$	304.9783	1.89	0.83	7.69	BD	Surratt et al., 2008
$C_8H_{14}O_{10}S$	301.0235	0.73	0.57	4.16	BD	Surratt et al., 2007
$C_5H_{10}O_{11}N_2S$	304.9783	1.56	0.42	2.90	BD	Surratt et al., 2008
$C_{10}H_{18}O_7S$	281.0701	1.03	0.33	6.76	BD	Riva et al., 2016
$C_5H_{10}O_{11}N_2S$	304.9783	3.60	0.31	3.32	BD	Surratt et al., 2008
$C_5H_9O_{13}N_3S$	349.9783	5.90	0.19	2.04	BD	Ng et al., 2008
$C_{10}H_{18}O_8S$	297.0650	0.75	0.14	5.25	BD	Riva et al., 2016
$C_5H_{11}O_8NS$	244.0133	1.93	0.11	1.46	BD	Nestorowicz et al., 2018
$C_5H_9O_{13}N_3S$	349.9783	5.49	0.02	0.17	BD	Ng et al., 2008
$C_5H_9O_{13}N_3S$	349.9783	5.34	0.008	0.10	BD	Ng et al., 2008
$C_5H_{12}O_8S$	231.0180	0.75	0.005	0.50	BD	Riva et al., 2016
$C_{10}H_{20}O_9S$	315.0755	1.46	0.002	0.21	BD	Riva et al., 2016

https://doi.org/10.5194/acp-2019-929
Preprint. Discussion started: 23 October 2019

Atmospheric Chemistry and Physics Discussions

Table 2. Comparison of concentrations of iSOA tracer concentrations and ratios in previous studies in the Amazon, SE USA and China. *Selected sample not an average concentration.

Location		China Urban, Beijing (2017)	China Rural, NCP (2013)	China Regional, Beijing (2016)	China Regional, PRD (2008)	SE US, Atlanta (2015)	SE US, Look Rock (2013)	SE US, Look Rock (2013)	SE US, Centreville (2013)	Amazon, T3 (2014)	Amazon, Manuas (2016)
Mean Concentration (ng m^{-3})	**2-MT**	17.3	44		91.5		861*	163.1			137*
	2-MT-OS	11.8		5.3	2.2	1792	2334*	169.5	217	83(wet)/ 399(dry)	390*
	2-MG	7.2	19.3		7.7			7.5			
	2-MG-OS	21.5		3.6	1.4	53		10	10.7	0.7(wet)/ 30(dry)	
Ratio low to high NO	**2-MT:2-MG**	2.40	2.30		11.9			21.7			
	2-MT-OS:2-MG-OS	0.55		1.47	1.57	33.8		17.0	20.3	118(wet) / 13(dry)	
Ratio CHO:CHOS	**2-MT:2-MT-OS**	1.47			41.6		0.37	0.96			0.35
	2-MG:2-MG-OS	0.33			5.51			0.75			
	Reference	This work	Li et al., 2018	Wang et al., 2018	He et al., 2018	Hettiyadura et al., 2019	Cui et al., 2018	Budlisulistiorini et al.,	Riva et al., 2019	Glasius et al., 2018	Cui et al., 2018